UNIVERSITY OF OKLAHOMA

GRADUATE COLLEGE

QUANTIFYING HYDRAULIC CONDUCTIVITY IN MINE DRAINAGE PASSIVE TREATMENT SYSTEM VERTICAL FLOW BIOREACTORS

A THESIS

SUBMITTED TO THE GRADUATE FACULTY

in partial fulfillment of the requirements for the

Degree of

MASTER OF ENVIRONMENTAL SCIENCE

By

BRYAN JOHN PAGE
Norman, Oklahoma
2016

QUANTIFYING HYDRAULIC CONDUCTIVITY IN MINE DRAINAGE PASSIVE TREATMENT SYSTEM VERTICAL FLOW BIOREACTORS

A THESIS APPROVED FOR THE
SCHOOL OF CIVIL ENGINEERING AND ENVIRONMENTAL SCIENCE

BY

_____
Dr. Robert W. Nairn, Chair

_____
Dr. Gerald A. Miller

_____
Dr. Robert C. Knox

Acknowledgements

I would like to thank my committee for the positive feedback and help throughout this process. Additionally, I would like to thank the 2014-2016 members of the Center for the Restoration of Ecosystems and Watersheds for helping collect data during long difficult field days. Finally, I would like to thank my parents, John and Carol Page.

Table of Contents

List of Tables

List of Figures

1 Introduction

1.1 Mining Influenced Waters

Heavy industrial mining has occurred in the United States for more than 100 years, and in many cases, has led to large-scale environmental degradation, especially from historical operations where mining occurred prior to environmental regulations (USDA 1993). Discharges of degraded water issuing from derelict or abandoned operations in the coal and hard-rock mining regions of the United States have substantial impacts on the environment. Many of these abandoned mine discharges (AMD) produce ecotoxic, metal-contaminated waters that have impaired receiving stream water quality and negatively impacted local ecology (Letterman and Mitch 1970; Younger et al. 2004).

According to data provided by USDA (1993), the United States Forest Service and Bureau of Mines estimated that 8,000-16,000 km of streams, in the eastern U.S. alone, had been impacted by mine drainage. Many of those stream kilometers are essentially biologically dead and may contain accumulated metal oxides, which can color the stream orange-yellow. The coloration is from the precipitation of dissolved iron as ferric oxyhydroxides and is locally referred to as “yellow boy”. Besides iron oxides, other metal contaminants of concern in coal mine drainage are manganese and aluminum, and there is a suite of trace metals (e.g., zinc, cadmium, lead) and water quality metrics (e.g., pH, alkalinity) that may pose ecological issues from hard-rock mines (Nairn et al. 2010; Younger 2000).

Varying types and degrees of AMD contamination exist. However, AMD can be broadly divided into two main types: net-alkaline and net-acidic. Alkalinity is a metric of how much acidity can be neutralized for a given quantity of water. Net-alkaline water has

available alkalinity after complete oxidation and hydrolysis of selected metals present in the water. In contrast, water is considered net-acidic if insufficient alkalinity is present to neutralize the available proton acidity and/or that produced by metal hydrolysis. Determining if the water is net-alkaline or net-acidic is critical to determination of viable treatment approaches and if alkaline addition is needed (Hedin et al. 1994).

Proper measurement of alkalinity and acidity is critical to identify if the water is net-alkaline or net-acidic. Determining pH and metals concentrations is important in determining net alkalinity or acidity. The oxidation and hydrolysis of certain metals can generate proton acidity. The generation of proton acidity makes AMD that may discharge alkaline become acidic. Some net-acidic AMD waters discharge with a pH in the ~2-3 range, but can be as low as -3.4 (Gazea et al. 1996; Nordstrom et al. 2000).

However, not all mine drainages have suppressed pH. Some AMD issuing from historical and active mining operations have a pH of 5-8 and are net-alkaline (Jageman et al. 1988; Nuttall and Younger 2000; Nairn 2010) due to the presence of carbonate geology. The effects of metal precipitation can be such that AMD discharges with a circum-neutral pH (pH ~5-6) can still be net acidic.

1.2 Literature Review

1.2.1 Treatment Options

Primarily, there are two different types of treatment methods for mining impacted waters: active and passive treatment. Active treatment relies heavily on the use of aggressive, highly alkaline industrial chemicals (e.g., lime, hydrated lime, soda ash, sodium-hydroxide, or ammonia), fossil fuels, and almost daily operation and maintenance. The added chemicals increase the pH of water so the dissolved metals readily precipitate

as oxide or hydroxide solids. The solids are flocculated and separated from the water in clarifiers/oxidation ponds to form sludge. Sometimes, additional mechanical aeration is provided. The retained sludge is pumped to a drying bed to remove excessive moisture. A substantial portion of the costs associated with active treatment are related to operation and maintenance, treatment chemicals, and sludge handling (Younger et al. 2002).

Passive treatment systems (PTS) are designed to use relatively little fossil fuels, natural physicochemical (e.g., limestone dissolution), and biological (e.g., bacterial sulfate reduction) processes for the treatment of AMD (Hedin et al. 1994, Fennessy and Mitsch 1989). The AMD is passed through, via gravity, a succession of treatment cells that are designed with specific treatment goals. Table 1-1 lists the variety and functionality of different cells that have been used in passive treatment systems. In the treatment of net-acidic waters, where additional alkalinity is needed, one of the key processes of passive treatment systems is alkalinity generation. These specific units include anoxic limestone drains, open limestone channels, automatically flushing limestone beds and various other geochemically-based systems, and vertical flow bioreactors (VFBRs). VFBRs utilize the dissolution of limestone to generate alkalinity for neutralization of excess protons and promote sulfate-reducing bacteria for trace metal removal as sulfides. The remainder of this document focuses on VFBR performance and operation.

Table 1-1 Different passive treatment cells and associated functions (Doshi 2006; Ziemkiewicz et al. 1997; Watzlaf et al. 2000)

Cell	Function
Vertical flow bioreactor (VFBR)	Alkalinity generation via anoxic limestone dissolution and metal retention via sulfate reduction
Anoxic limestone drain	Alkalinity generation via anoxic limestone dissolution
Oxidation ponds	Oxidation, hydrolysis, precipitation, and retention of metals
Open limestone channels	Oxidation, precipitation, and retention of metals
Surface flow wetlands	Oxidation, precipitation, and retention of metals
Horizontal flow limestone beds	Manganese and zinc retention and alkalinity generation via limestone dissolution
Automatic flushing limestone beds	Alkalinity generation via limestone dissolution

1.2.2 Vertical Flow Bioreactors

The exact composition of individual VFBRs will vary from system to system, but will generally consist of an organic substrate, alkaline substrate, collection system, and water level control structure. Figure 1-1 shows a typical cross section of a VFBR during normal operation. The AMD flows into the VFBR on the left (A). The water level (B) is maintained above the treatment media (C), to maintain anoxic conditions and to limit vegetation growth in the VFBR. The water then passes vertically through the treatment media and is gathered by the collection system (D) (Johnson and Hallburg 2005). The elevation of the treated effluent control structure (E) from the VFBR maintains water levels. Water continues to the next cell, typically a reaeration pond. For operation and maintenance issues and if site conditions allow, VFBRs typically have a flush valve (F) so that the system can be drained and accumulated inorganic and organic solids flushed.

The degradation of organic material under anoxic conditions provides the necessary environment for sulfate reducing bacteria (SRB). Based upon availability and distance from the source, several organic materials have been used in VFBR substrates, including, but not limited to, composted horse manure, mushroom compost, composted chicken litter, hay and straw, waste recycled paper, and municipal compost (Chang et al. 2000; Nairn et al. 2010; Dvorak et al. 1992). The alkaline substrate, typically mixed with the organic material, is used to improve the hydraulic conductivity and provide additional treatment by dissolution. The alkaline substrate generally consists of limestone, but dolomite, and mussel and arthropod shells have been used (Hengen et al. 2014). The nominal size of the substrate materials used within VFBRs can vary from a few millimeters to several centimeters in diameter. The wide variety of materials within the VFBRs makes the identification of substrate material critical when determining performance over time.

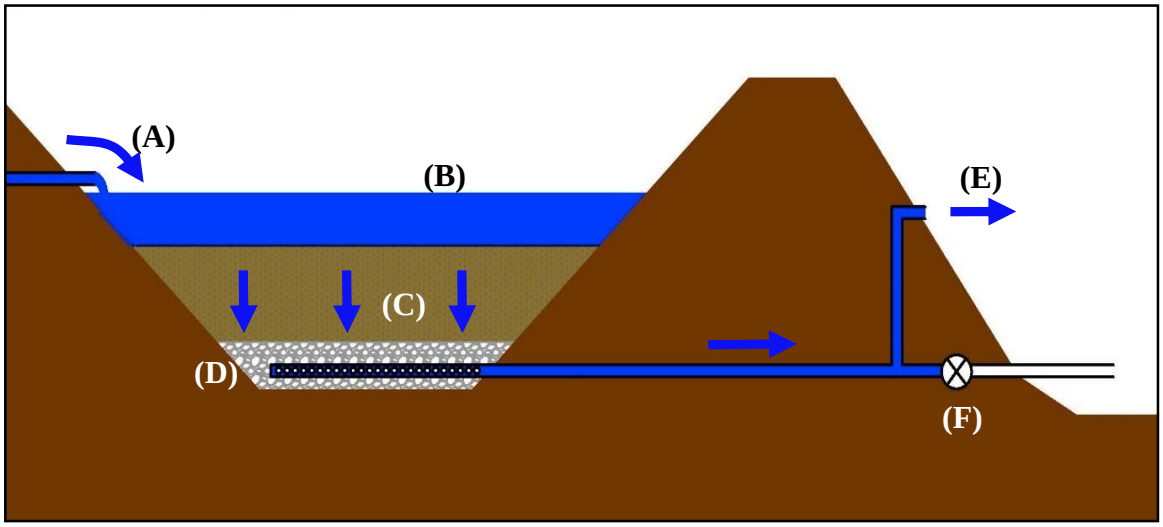

Figure 1-1 Typical cross section a VFBR under normal operating conditions.

The collection system, which acts as the drainage layer, consolidates the treated water from the substrate to discharge to the next treatment cell. Typically, the collection system will consist of a series of perforated drain pipes in a bed of non-reactive bedding

material. The bedding material generally consists of rounded sandstone. A non-reactive bedding material is used to reduce the formation of metal precipitates near the drain pipe, which may lead to scaling, plugging or other hydraulic conductivity problems. The perforated drain pipe can vary in size and material. Generally, polyvinyl chloride (PVC), or high density poly-ethylene (HDPE) pipes are used due to the reactiveness of the water.

The design life of VFBRs is generally several decades (e.g., Gusek 2002). Maintaining appropriate and accurate water elevations in a VFBR is critical to successful treatment. Many different types of flow control structures exist, but typically a peri-pipe or stop-log system is utilized. A peri-pipe system is an adjustable outlet that uses different size pipes and a flexible rubber coupling. A stop-log system controls the water elevation by the addition or removal of non-reactive boards, either fiberglass reinforced polyester or PVC. If adequate elevation change exists, a flush valve is typically added so the system can be drained for maintenance issues.

1.2.3 Hydraulic Conductivity

Long term operation and maintenance issues arise in many ways and in different treatment cells. One of the key maintenance issues associated with VFBRs is decreased hydraulic conductivity, which leads to either water by-passing the cell or decreased treatment efficiencies (Demchak et al. 2001; Denholm et al. 2010; Doshi et al. 2006). If hydraulic conductivity issues are not addressed, the passive treatment system effluent may stop meeting treatment goals.

The Filson 1 PTS treats an AMD in Jefferson County, Pennsylvania. The PTS was constructed in 1994 and included two cells similar to the above described VFBRs just by another name: successive alkaline producing systems (SAPS). After only three years of

operation, it was noted that approximately 50% of the flow was by-passing the SAPS, but the cell was still able to positively impact the total pollution load (Demchak et al. 2001). The PTS was tested for functionality over a 12-month period from 1996 to 1997 (Demchak et al. 2001). By May 1999, both the flow and treatment in the cells decreased to the point that the cells had to be rehabilitated to return the original functionality (Damariscotta 2003).

The Jennings PTS in Butler County, Pennsylvania has been a demonstration site for various innovative passive treatment technologies since 1989. In 1997 a VFBR was constructed to treat AMD. By 2004 the permeability of the VFBR had decreased to the point that the majority of water was by-passing the cell and not being treated (Denholm et al. 2010). During that same year, the organic treatment media of the VFBR was mechanically mixed, which increased the hydraulic conductivity of the substrate. Within three years the hydraulic conductivity of the VFBR decreased again and the cell was mixed once more in 2007 (Denholm 2010). During this time, all of AMD that passed through the substrate was being adequately treated, but since a majority of the water was by-passing the cell, the entire AMD flow was not getting effectively treated (Denholm et al. 2010). The VFBR was overhauled completely in 2012 and full functionality of the VFBR was restored (Dunn et al. 2014).

In Reynolds County, Missouri at the West Fork Mine Site, a VFBR was constructed in 1996 to treat a discharge from an active lead-zinc mine (Gusek et al. 1998). The VFBR experienced a number of hydraulic conductivity problems related to geotextile layers, algal mat growth and suspended solids entering the cell. Eventually, woodchips were added to the treatment mix in order to increase the hydraulic conductivity (Doshi et al. 2006).

Even with issues in aging VFBRs, there is a dearth of hydraulic conductivity measurements for treatment substrates. The few studies that have been done are based upon tracer studies and were conducted on systems that had been in operation for four years or less (Diaz-Goebes and Younger 2004; Wolkersdorfer et al. 2005; Watson et al. 2008).

In 2000, Diaz-Goebes and Younger did a tracer study on the newly built Bodwen Close PTS and at the Pelenna III PTS, which was built in 1998. At the Bodwen Close PTS, 1-kg of LiCl was used as tracer on a VFBR with a treatment mix of composted conifer bark mulch, cow manure, and straw. The hydraulic conductivity of the new system was estimated to be $3x10^{-3}$ cm/s. For the two-year old system at Pelenna III, a similar tracer study was completed with 50-kg of NaCl. The treatment substrate was composed of composted manure and straw. The determined hydraulic conductivity was $3.6x10^{-4}$ cm/s (Diaz-Goebes and Younger 2004). In 2004, additional tracer studies were completed at the Bowden Close PTS and the updated conductivity was estimated to have decreased to $4x10^{-4}$ cm/s. No hydraulic conductivity issues were noted during testing (Wolkersdorfer et al. 2005).

At the Tan y Garn abandoned coal mine in South Wales, UK, a PTS was built in 2006. Watson et al. (2008) monitored the hydraulic conductivity of the system over the first two and one-half years of operation. The treatment media in the VFBR was layered with 10 cm of municipal compost, 60 cm of mixed layer of 50:50 municipal compost and limestone gravel, and 10 cm of limestone gravel, from top to bottom, respectively. At the startup of the VFBR the hydraulic conductivity was reported to be $6x10^{-3}$ cm/s. After, one year of operation the hydraulic conductivity decreased to $1x10^{-3}$ cm/s and by the second year of the study it had decreased to $2x10^{-4}$ cm/s (Watson et al. 2008).

1.3 Objectives and Hypotheses

This research focused on characterizing the organic layer in VFBRs and quantifying the hydraulic conductivity of multiple passive treatment systems with the intention of developing plans for extending the lives of the treatment systems. The first objective for this research was to show that the hydraulic conductivity values of the VFBRs have changed since installation, therefore requiring operation and maintenance to maintain water quality improvement performance. The second objective was to compare several different methods of determining hydraulic conductivity and expected values.

The first hypothesis for this research is the hydraulic conductivity and other physical characteristics of the treatment substrate that has been in operation for an extended period of time differ significantly from those determined by the available data obtained before or during the installation of the VFBRs. The second hypothesis was that a comparison of several different methods, including the new method, of determining hydraulic conductivity will return statistically similar results.

2 Methods

2.1 Site Selection

The first step of site selection was identification of appropriate passive treatment systems with VFBRs. Prior to field work, information and data were collected (e.g., available as-built designs, water quality performance data) about each of the identified sites. Based on the available information and data, the Mayer Ranch, Hartshorne and Red Oak PTS were selected for this study.

2.1.1 Selected Sites

The three selected sites are located in eastern Oklahoma (Figure 2-1). Hartshorne and Red Oak PTS are located in the Arkoma Basin where bituminous coal was, and still is, mined (Suneson 2012). The Mayer Ranch PTS is located in northeast Oklahoma, within the Tar Creek Superfund Site, part of the Tri-State Lead-Zinc Mining District.

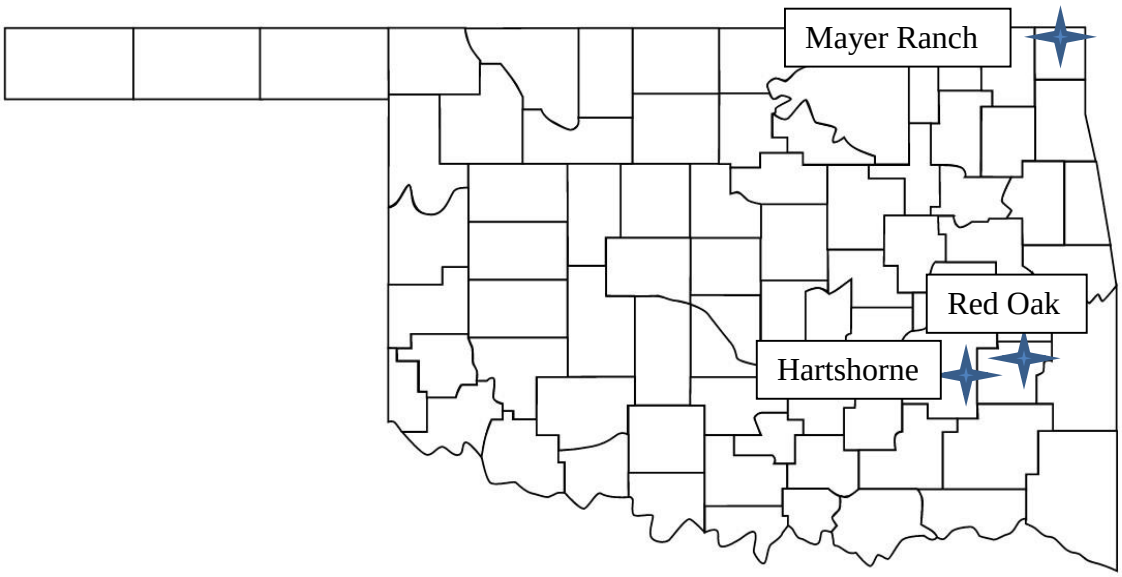

Figure 2-1 Location map of the three selected sites.

A summary of the locations and other basic information about the selected PTS is in Table 2-1. The original AMD issuing from the abandoned mining operations in the Arkoma Basin (Hartshorne and Red Oak PTS) are net acidic, while at Mayer Ranch PTS, the AMD discharge is net alkaline. The raw mine water at these three locations has elevated levels of metals and suppressed pH. A summary of raw water for the selected PTS is in Table 2-2.

Table 2-1 Comparison of selected PTS.

PTS	Location	Number of Cells	Type of Mining	Net Alkaline/ Net Acidity
Mayer Ranch	Ottawa County, OK (Tar Creek Superfund Site)	10	Lead/Zinc	Alkaline
Red Oak	Latimer County, OK (Arkoma Basin)	5	Bituminous Coal	Acidic
Hartshorne	Pittsburg County, OK (Arkoma Basin)	5	Bituminous Coal	Acidic

Table 2-2 Raw water quality for selected PTS (Nairn et al. 2010, Canty 1999)

PTS	pH	Fe (µg/L)	Al (µg/L)	Mn (µg/L)	Zn (µg/L)	Pb (µg/L)	Cd (µg/L)	Ni (µg/L)
Mayer Ranch	5.9	192,000	-	1,200	11,000	60	17	970
Red Oak	4.4	200,000	6,000	7,000	360	<1	<1	308
Hartshorne	5.4	765,000	351	11,000	43	180	17	110

2.1.2 Mayer Ranch PTS

The Mayer Ranch PTS was constructed in 2008 to ameliorate a net alkaline discharge from the historic lead-zinc Tri-State Mining District (Nairn 2010). The treatment system is comprised of ten treatments cells, with eight (C2N/S-C5N/S) in parallel treatment trains of four cells (Figure 2-2). C3N and C3S are the VFBRs and were selected for testing. Summary influent water quality for Mayer Ranch PTS is in Table 2-2. The degraded mine water is similar to other AMD discharges in the Tri-State Mining District (Nairn 2010).

The VFBRs at Mayer Ranch PTS and are comprised of mixed organic treatment media, limestone drainage layer, and inline water level control structure from Agri Drain. The treatment media was composed of 10% limestone sand, 45% compost, and 45% woodchips. In addition, the Mayer Ranch PTS VRBRs were constructed with horizontal porewater samplers. The porewater samplers are grouped into three different locations within each cell and the samplers extend different distances (Figure 2-3).

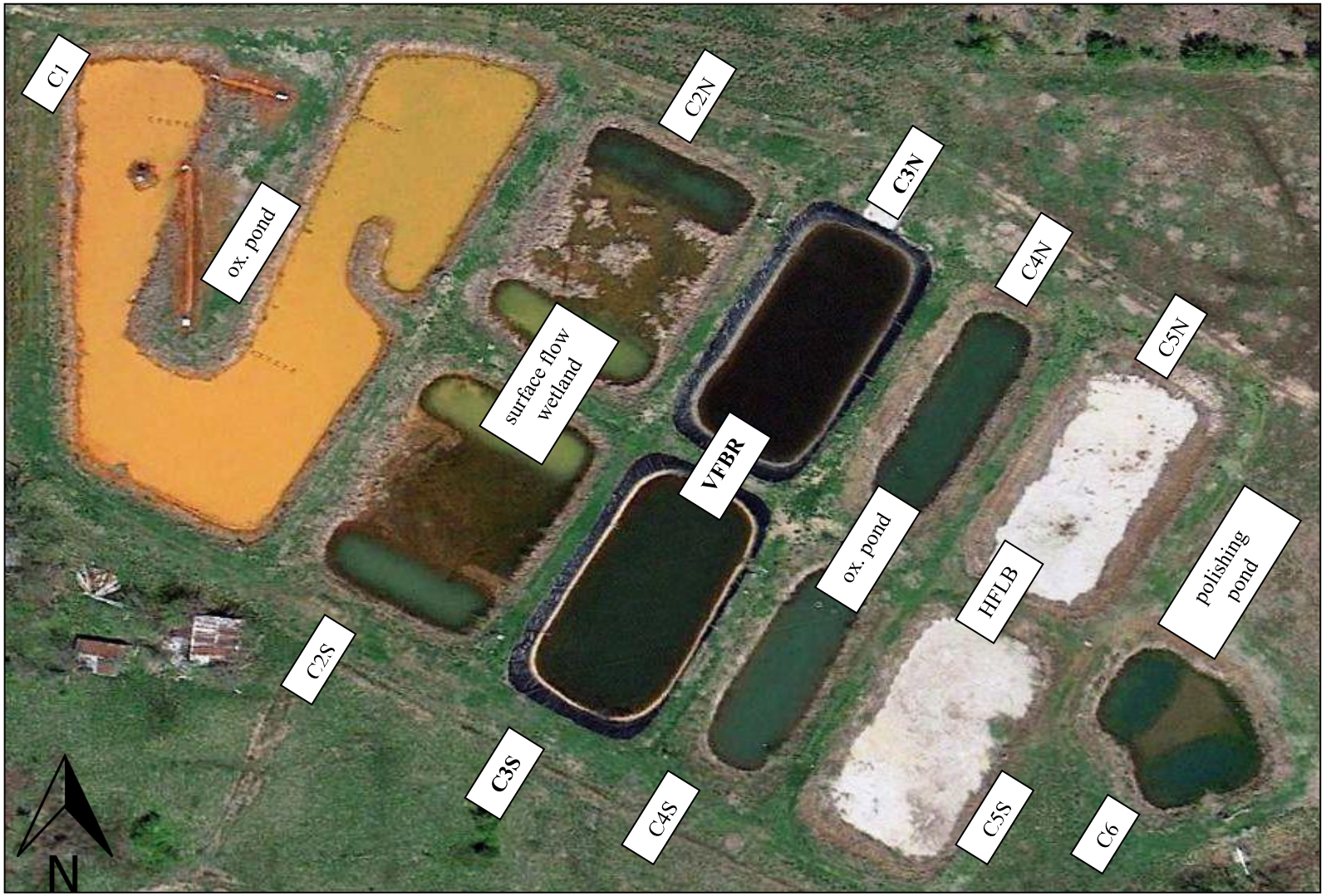

Figure 2-2 Aerial imagery of Mayer Ranch PTS. (Google Earth A 2013)

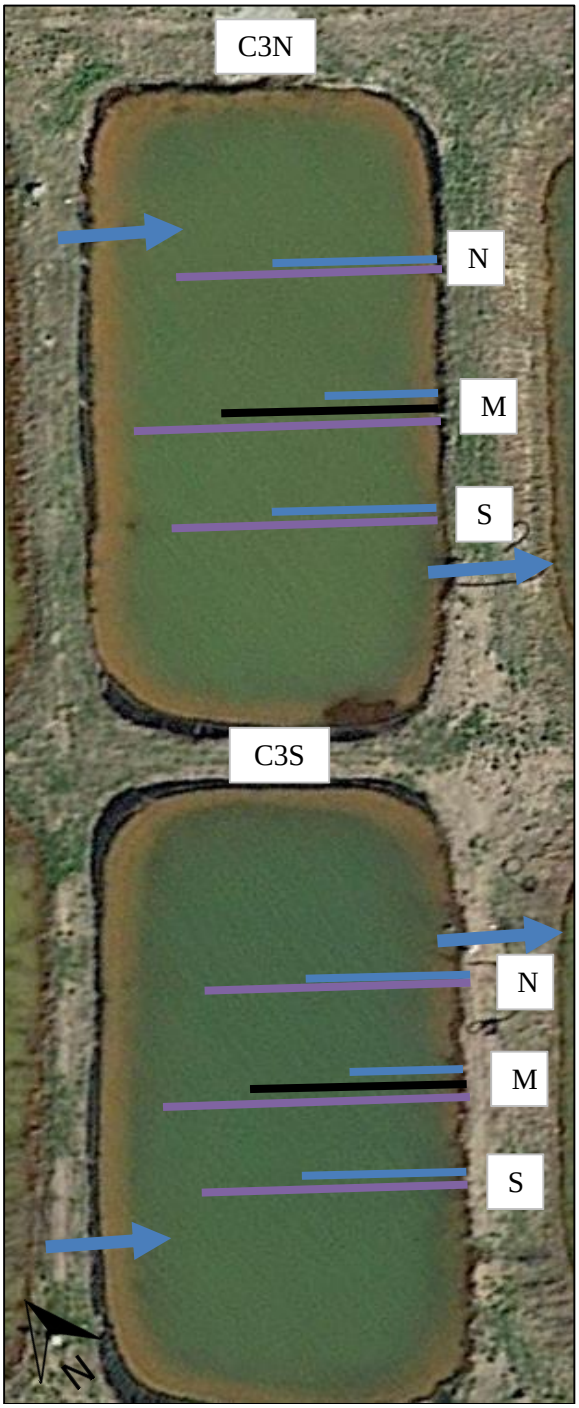

Figure 2-3 Diagram of the porewater samplers at Mayer Ranch PTS. The length of the porewater samplers are not to scale. Locations are approximate. The blue arrows indicate where the water enters and leaves the cell. (Google Earth A 2013)

2.1.3 Red Oak PTS

The Red Oak PTS was constructed in 2001 to address a net acidic discharge from an abandoned bituminous coal mine in the Arkoma Basin. The treatment system is comprised of 5 cells (Figure 2-4). C2 and C4 are VFBRs, but only C4 was selected for testing due to a malfunctioning flush valve for C2. A summary of the influent water quality for Red Oak PTS is in Table 2-2. The degraded mine water is similar to other AMD in the Arkoma Basin.

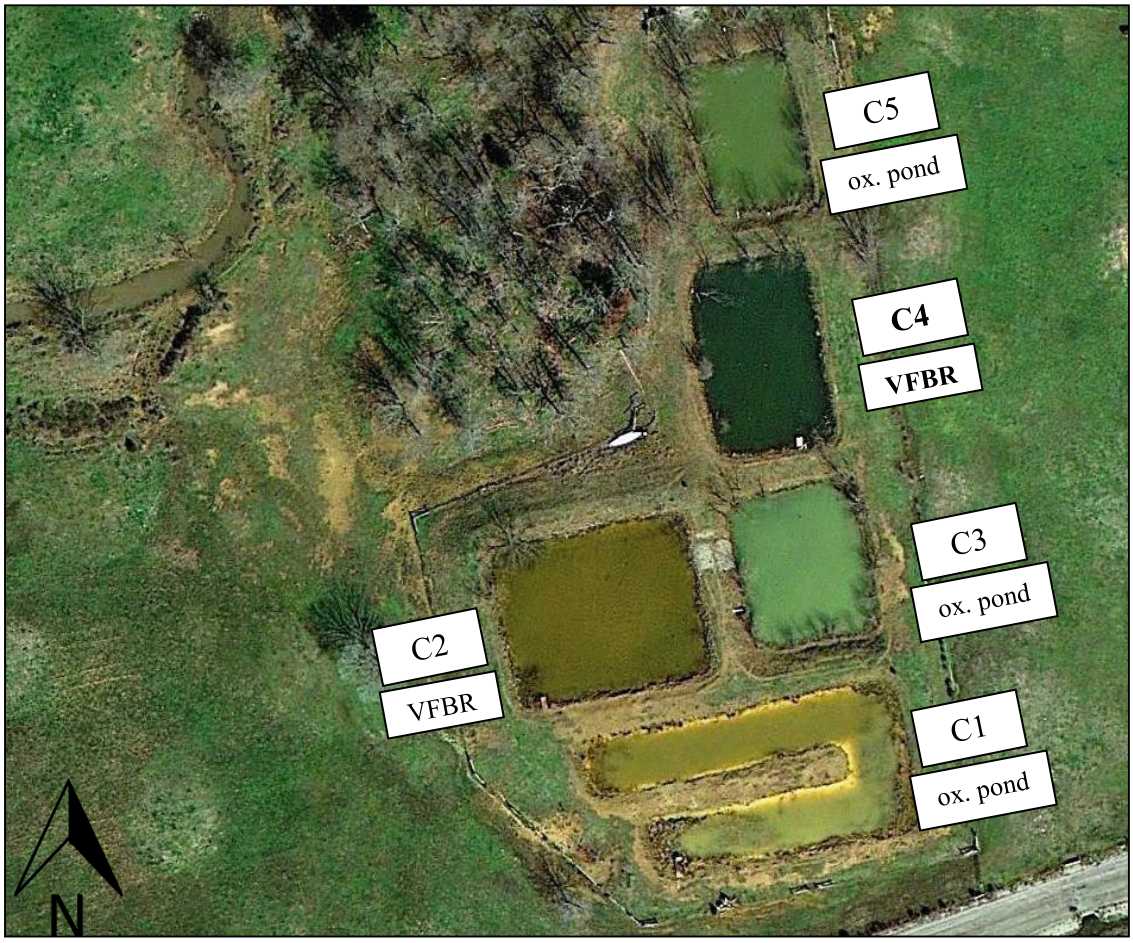

Figure 2-4 Aerial image of Red Oak PTS. (Google Earth B 2013)

C4 is comprised of an organic treatment media mix, limestone drainage layer, effluent control structures and a flush valve. During the construction of Red Oak PTS, nested piezometers were installed in C4. At Red Oak PTS, the treatment media is composed

of limestone gravel and stable waste. The location of nested piezometers is shown in Figure 2-5.

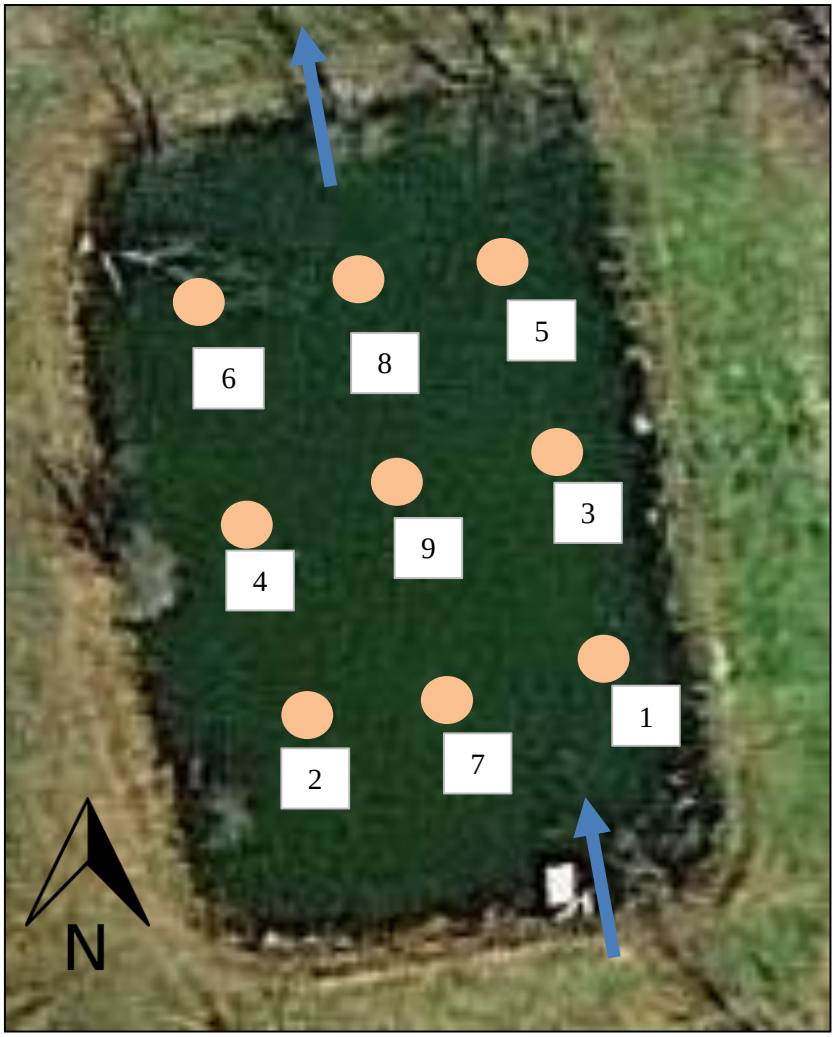

Figure 2-5 Diagram of the nested piezometer at the Red Oak PTS. Locations are approximate. The blue arrows indicate where the water enters and leaves the cell. (Google Earth B 2013)

2.1.4 Hartshorne PTS

The Hartshorne PTS was constructed in 2005 to address a net acidic discharge from an abandoned bituminous coal mine in the Arkoma Basin. Similarly, to Red Oak PTS, the treatment system is comprised of 5 cells (Figure 2-6). C2 and C4 are VFBRs, but only C4

was selected to be tested. A summary of the influent water quality for Hartshorne PTS is in Table 2-2.

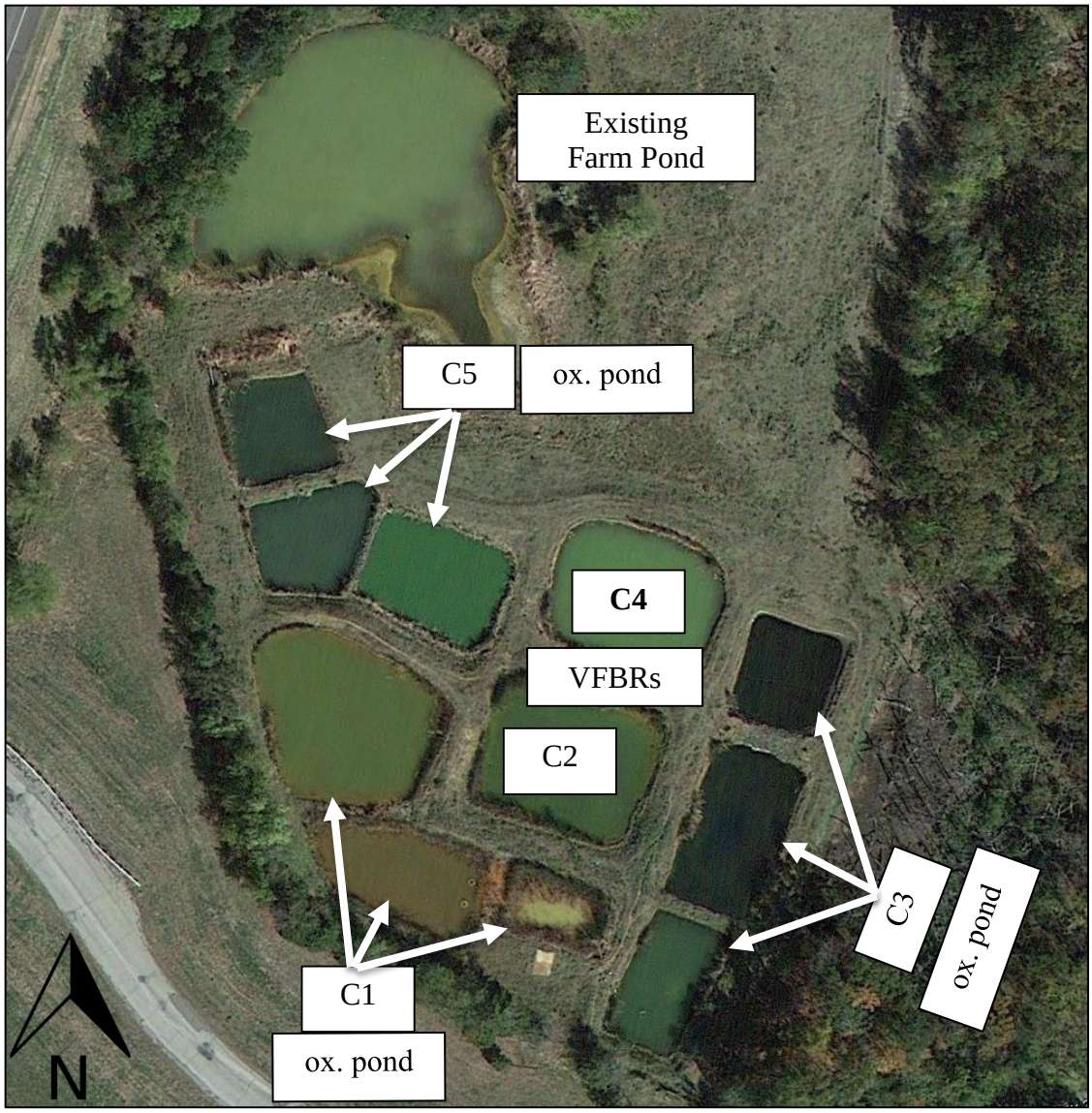

Figure 2-6 Aerial image of Hartshorne PTS. (Google Earth 2012)

C4 is different than the other selected VFBRs in that the treatment media is layered. A layer of 100% spent mushroom compost overlays a layer of limestone. The VFBR is comprised of an organic treatment layer, limestone drainage layer, effluent control structures and a flush valve. No additional piezometers or porewater samplers were installed during construction. The system may have been constructed in late 2005, but due

to a severe regional drought AMD did not flow through the system until early 2007. During that time, a portion of berm eroded into the treatment substrate and may have impacted the hydraulic conductivity of the VFBR. Since the AMD did not begin to flow through the system until 2007 that will be the year noted as when the system begun operation. Figure 2-7 shows where the water enters and exits the cell.

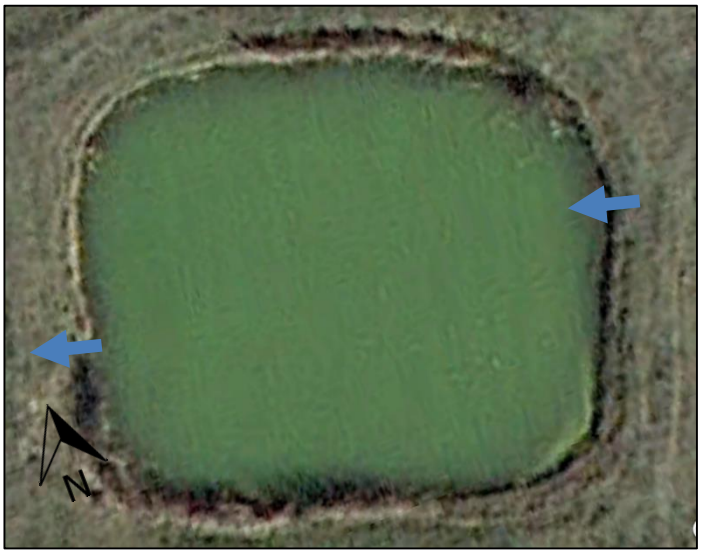

Figure 2-7 Aerial photograph of the VFBR at the Hartshorne PTS. The blue arrows indicate where the water enters and leaves the cell. (Google Earth 2012)

2.1.5 Summary of Selected VFBRs

Various features of the selected VFBRs are summarized in Table 2-3. The VFBRs are similar in basic construction, for example the use of an organic substrate in the treatment mix, but differ in types of treatment media, hydraulic loading rate, configuration, surface area, and other metrics.

Table 2-3 Summary of selected VFBRs

PTS	Mayer Ranch	Mayer Ranch	Red Oak	Hartshorne
Site abbreviation	C3N	C3S	RO	H
Cell studied	3N	3S	4	4
Treatment Media	10% limestone sand 45% wood chips 45% mushroom compost	10% limestone sand 45% wood chips 45% mushroom compost	stable waste limestone gravel	100% mushroom compost
Year Constructed	2008	2008	2001	2007
Treatment Media Surface Area (m^2)	604	556	388	202
Designed Thickness (m)	0.5	0.5	1.0	0.5
Volume (m^3)	302	278	388	101
Measured Thickness (m)	0.37	0.29	-	0.35
Design Flow (m^3/min)	0.237	0.237	0.0756	0.0389
Hydraulic Loading Rate (cm/s)	2.35E-02	2.56E-02	1.17E-02	1.16E-02

2.2 Field Methods

2.2.1 Field Falling Head Permeability Tests (F-FHT)

Full-scale falling head permeability tests were done for whole VFBRs, which is represents the hydraulic conductivity for the whole treatment unit. Pressure transducers (Solinst Model 3001) were deployed in various treatment cells (VFBRs and down-gradient process units) such that hydraulic conductivity could be calculated after VFBR drain valves were opened. With the transducers deployed, background water level data were collected for a minimum of 24 hours prior to performing full-scale falling head permeability tests. While the background data were collected, the relative elevations of the water levels and controlling discharge elevations (e.g., invert of the effluent pipes) were determined. These

measurements were utilized in determination of the hydraulic head between each cell. Once the initial elevation data were collected, the flush valve of the VFBR was opened allowing the VFBR to drain, thus providing for a full-scale falling head test. The flush valve remained open for a minimum of one week to either allow the system to completely drain to the substrate level or come to steady-state at a new water elevation.

$$K = \frac{aL}{At} \ln\left(\frac{h_o}{h_1}\right) \quad \text{(eq. 2-1)}$$

Where:

K = hydraulic conductivity

a = area of the VFBR water surface

L = length of the treatment media (depth of media)

A = area of the VFBR treatment media surface

h_0 = initial height of water

h_1 = final height of water

t = time required to get reach h_1 from h_0

2.2.2 Modified Single Ring Infiltrometer Test (MI)

An innovative single ring infiltrometer was developed specifically for this project. The infiltrometer represents the hydraulic conductivity of only the treatment media and is a point measurement. For the single ring infiltrometer test, the water level within the VFBRs was lowered to ~75-150 mm above the organic substrate surface. If the cell could not be drained to the appropriate level due to site conditions, the water was either pumped from the next component so the cell could drain or the water was pumped directly from the cell. A modified 25.4-cm diameter single ring infiltrometer was designed and built for this test. A scalloped band-saw blade was welded on the bottom of the steel infiltrometer so the

ring would cut through the material with minimal disturbance. The modified infiltrometer is 53.4 cm in length and was designed to go through the entire section of organic substrate at some locations. Seven centimeters from the base of the infiltrometer, a pre-drilled hole allowed installation of a manometer once the infiltrometer was placed to its final depth in the substrate.

As shown in Figure 2-8, the infiltrometer (A) was rotated into the organic substrate (B), minimizing disturbance. Once the bottom was placed at the appropriate depth, gym weights (totaling 57 kg) (C), a 151-cm PVC standpipe (D), a manometer (E), and a measuring tape (measuring down from the top of the stand pipe) were installed. A pressure

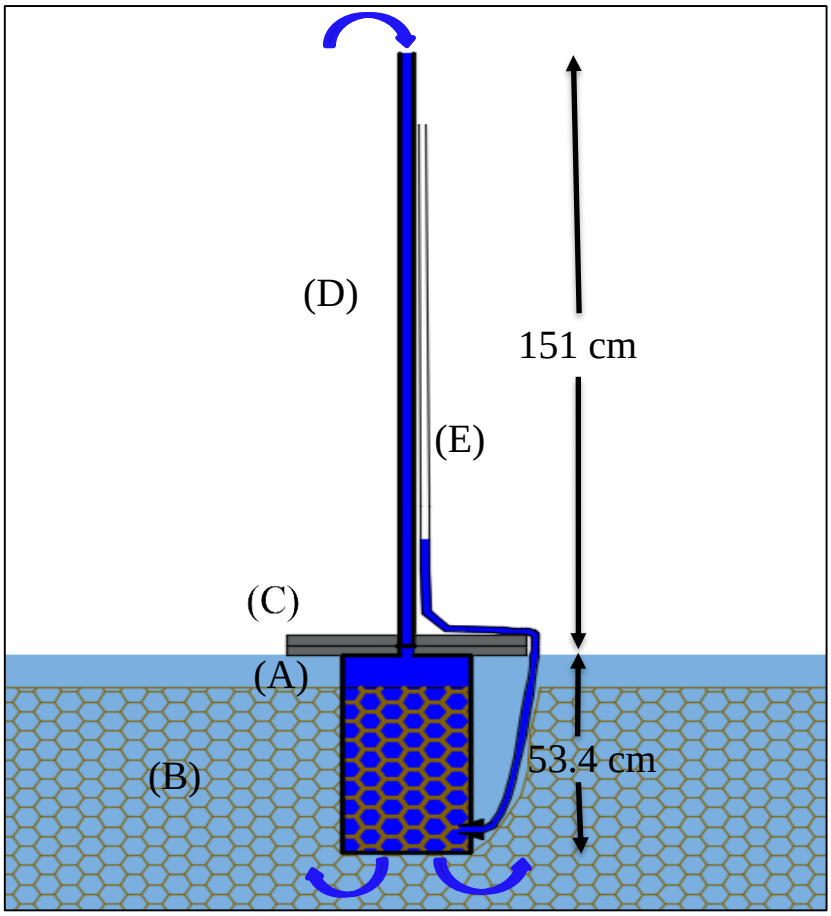

Figure 2-8 Diagram of the modified single ring infiltrometer during operation.

transducer was deployed in the standpipe to measure the water level at one second intervals. Water was then added to the infiltrometer to fill the standpipe.

The falling water levels within the standpipe and manometer were respectively monitored with the transducer as well as manually. This in-situ falling head test was repeated several times to gather a statistically valid set of measurements. Once the falling head infiltrometer tests were complete, the organic substrate was removed from the outside of the infiltrometer and a foam pad was slid into place on the bottom. Once the pad was in place, the infiltrometer was carefully removed and the substrate within the infiltrometer was collected for use in other tests. Two core samples were taken from each VFBR and returned to the laboratory. The calculations for the MI are the same calculations presented for the F-FHT.

At each selected VFBR, the MI was tested at least four different locations. The locations were distributed to get a representative value for the substrate layer. Figures 2-9 through 2-12 show the test locations for each of the selected PTS. Location MI-1 shown in Figure 2-12 was not included in the calculations since the methodology for the apparatus was still being developed.

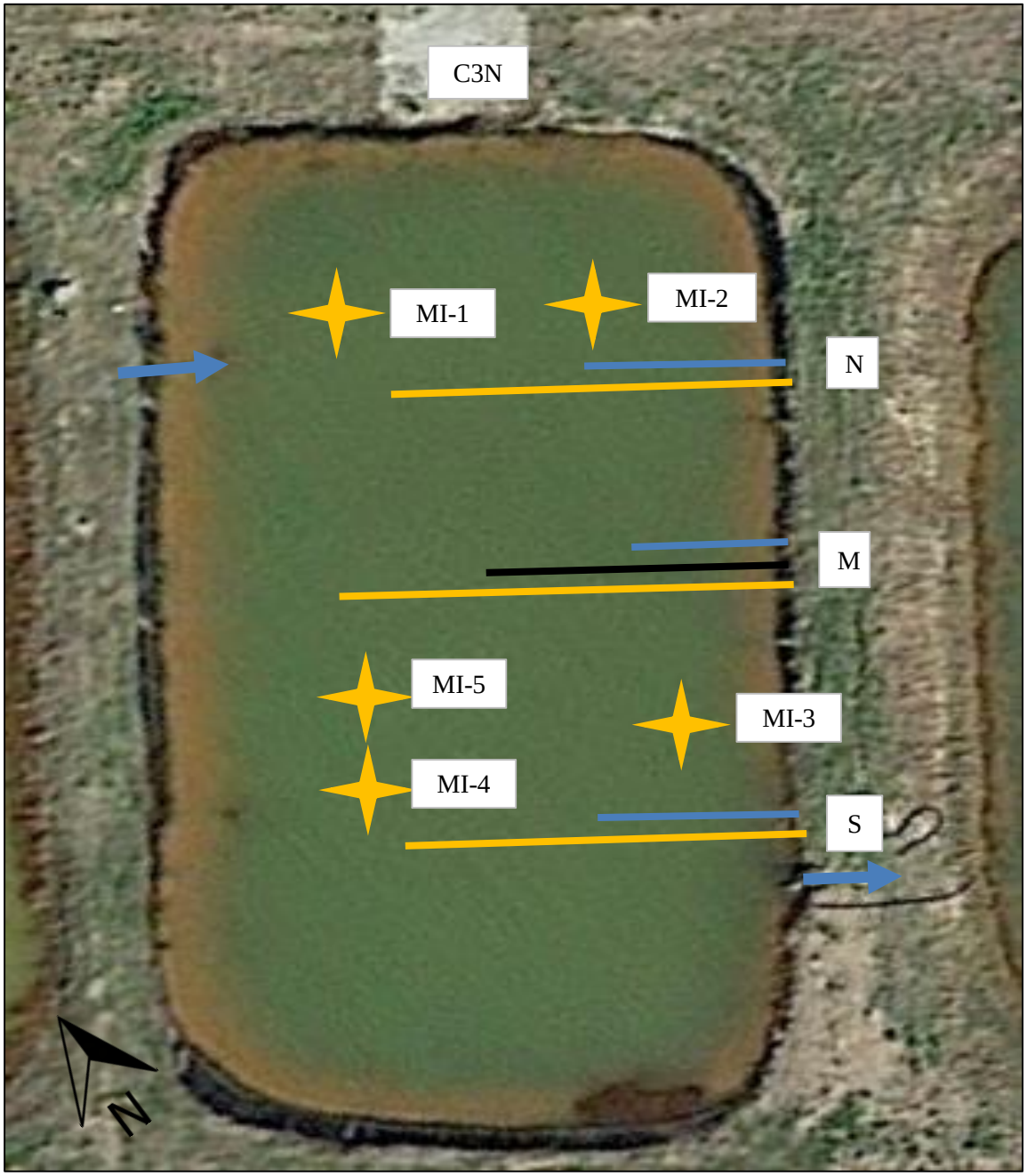

Figure 2-9 Diagram of hydraulic conductivity tests at Mayer Ranch PTS C3N. The yellow, black, and blue line indicated tested porewater samplers. The yellow stars indicate the locations of the MI tests. Locations are approximate. The blue arrows indicate where the water enters and leaves the cell. (Google Earth A 2013)

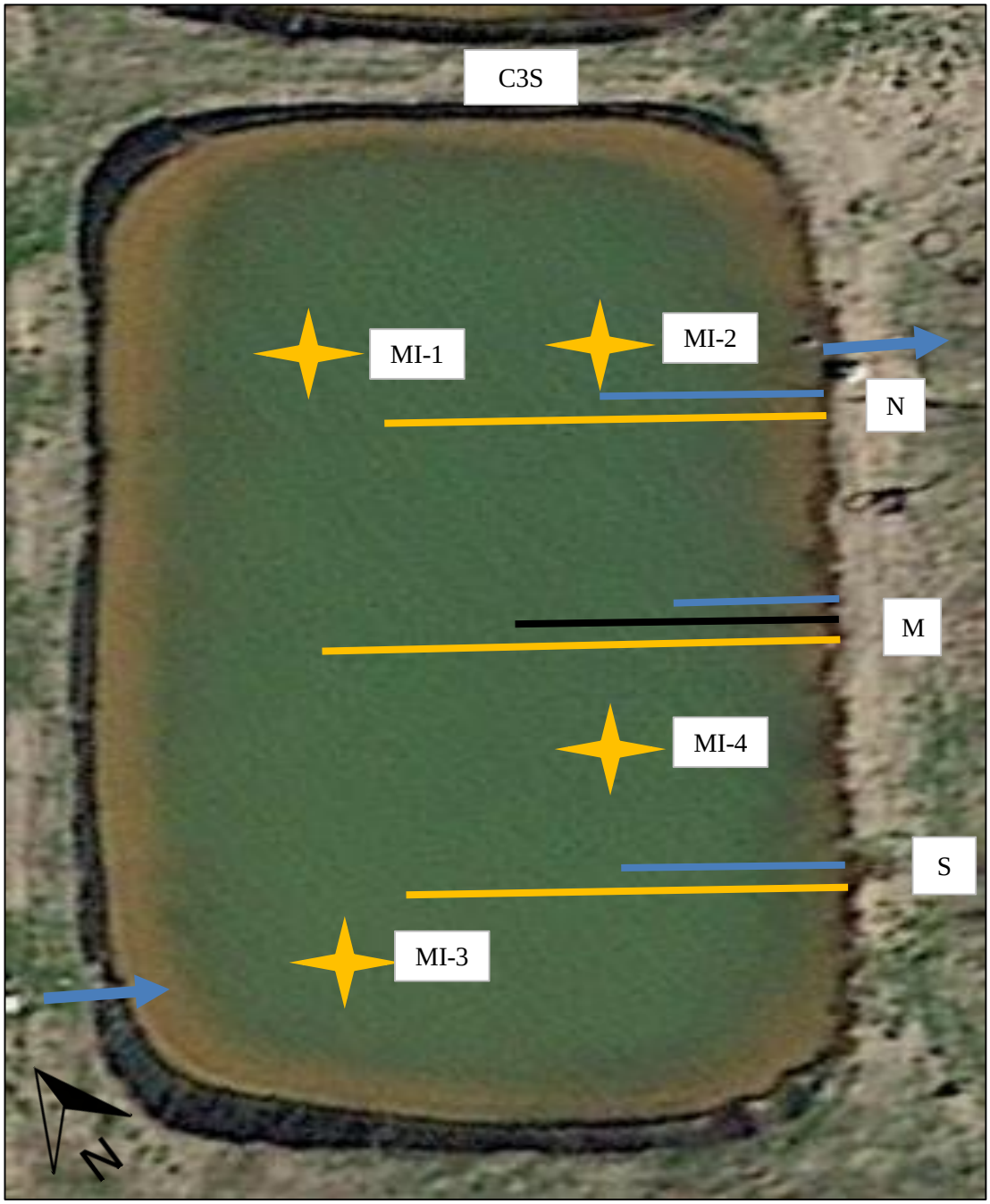

Figure 2-10 Diagram of hydraulic conductivity tests at Mayer Ranch PTS C3S. The yellow, black, and blue line indicated tested porewater samplers. The yellow stars indicate the locations of the MI tests. Locations are approximate. The blue arrows indicate where the water enters and leaves the cell. (Google Earth A 2013)

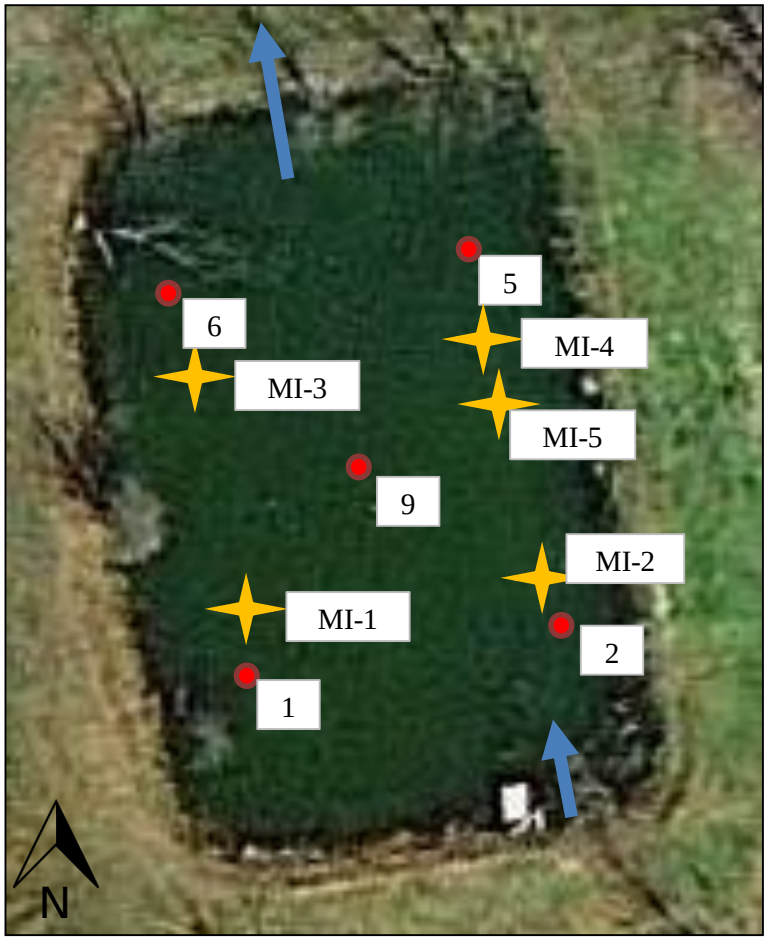

Figure 2-11 Diagram of locations for hydraulic conductivity tests at the Red Oak PTS. The red dots indicate locations where nested piezometers were tested and the yellow stars indicate the locations of the MI tests. Locations are approximate. (Google Earth B 2013)

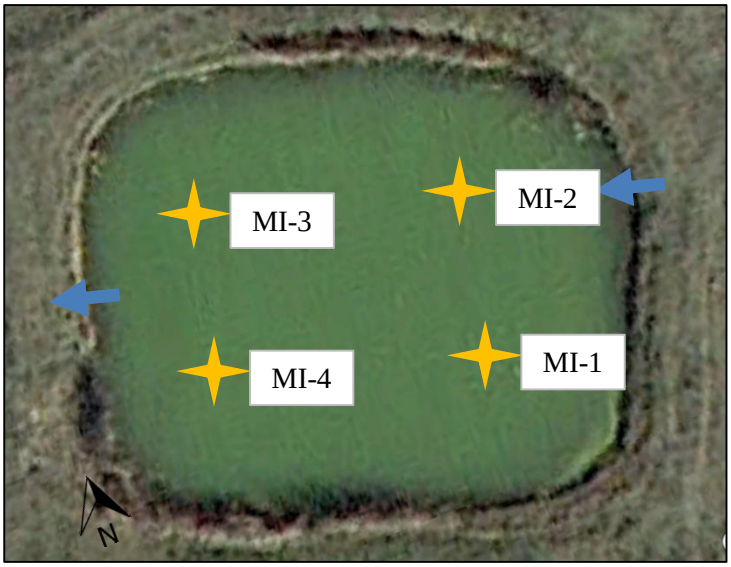

Figure 2-12 Diagram of hydraulic conductivity tests at Hartshorne PTS. The yellow stars indicate the locations of the MI tests. Locations are approximate. (Google Earth 2012)

2.2.3 Slug Tests (ST)

Mayer Ranch and Red Oak had previously installed pore water samplers and piezometers, but Hartshorne did not. The slug tests are point measurement of the treatment media and represent the hydraulic conductivity of only the treatment media around the casing. At Red Oak PTS, 18 piezometers were installed during construction. At each location, there are two piezometers installed at different depths: 0.3 and 1 m. The piezometers were installed with a 15.3-cm sand pack. Slug tests were performed on ten of the piezometers at Red Oak PTS following the Bouwer and Rice Slug Test Method for partially penetrating wells (Bouwer and Rice 1976). While the VFBRs were normal operation, a transducer was installed in the piezometer to measure the water elevation in the piezometer. A sufficient quantity of water was added to the piezometer to overflow the piezometer. This quantity of water acted as a "slug" and by monitoring the rate of decrease in the piezometer it was possible to calculate the hydraulic conductivity. Once the water returned to near steady-state (e.g., the original elevation in the piezometer), the test was repeated two more times. The transducer remained in the piezometer until the water level again reached near steady-state. The transducer was then retrieved for data collection.

At the Mayer Ranch PTS, horizontal porewater samplers were installed during the construction of the VFBRs. The porewater samplers consist of 0.64-cm diameter LDPE lines within 2.5-cm PVC electrical conduit. The screen interval of the porewater samplers are 68.6 to 71.2-cm. In each of the VFBRs, there are seven porewater samplers that extend 4.3, 5.7, 8.5, 11.4, and 12 m from shore into the VFBR substrate at a depth of approximately 23 cm.

For this study, an apparatus was attached to the existing porewater samplers (Figure 2-13). The apparatus was a 5.1-cm diameter by 1.5-m PVC pipe that was drilled and tapped such that a 0.64-cm diameter valve and a 0.64-cm diameter manometer could be threaded onto the pipe, 15-cm from the bottom of the pipe. The bottom of the pipe was capped with a 5.1-cm PVC cap. The 5.1-cm pipe had gradations on the side to measure the water level in the pipe, via the manometer. Water was added to the 5.1-cm diameter pipe and the water level in the pipe was monitored as it drained out through the porewater sampler.

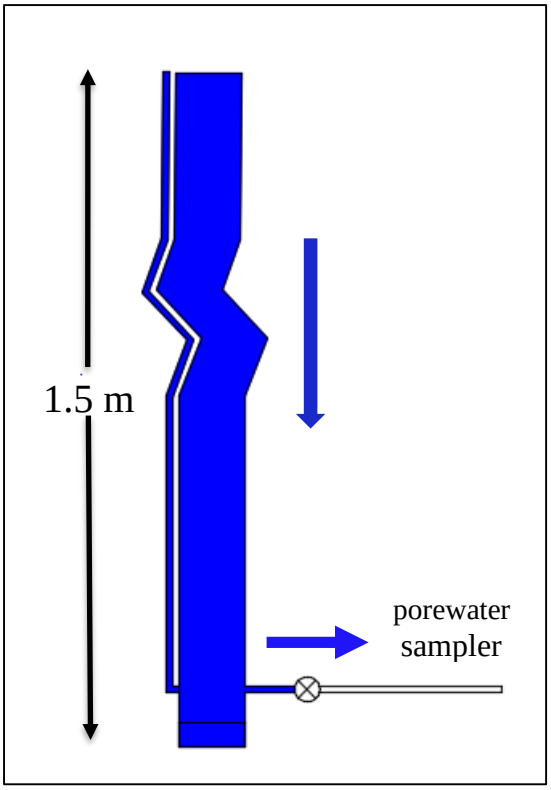

Figure 2-13 Diagram of the apparatus used to perform the slug test at Mayer Rach PTS.

By measuring the flow rate through the porewater samplers and comparing the hydraulic head between the VFBR and the apparatus, the hydraulic conductivity of the organic substrate surrounding the `porewater samplers was estimated. Below are the

equations used to calculate the hydraulic conductivity (Figure 2-14, 2-15), as shown in Bower (1989).

Bower and Rice Equations:

$$K = \frac{r_c^2 \ln\left(\frac{R_e}{r_w}\right)}{2L_e} \frac{1}{t} \ln\left(\frac{y_o}{y_t}\right) \quad \text{(eq. 2-2)}$$

where

$$\ln\left(\frac{R_e}{r_w}\right) = \left[\frac{1.1}{\ln\left(\frac{L_w}{r_w}\right)} + \frac{A + B\ln\left[\frac{H-L_w}{r_w}\right]}{\frac{Le}{r_w}}\right]^{-1} \quad \text{(eq. 2-3)}$$

$K =$ hydraulic conductivity around screened interval

r_c= radius of the pipe

r_w= radial distance of undisturbed portion from centerline

R_e= effective radial distance over which y is dissipated

L_e= screened interval

L_w= vertical difference between bottom of casing and static water table outside

$y =$ vertical difference between water level inside well and static water table outside

$y_0 = y$ at time 0

$y_t = y$ at time t

t= time

A, B = dimensionless numbers

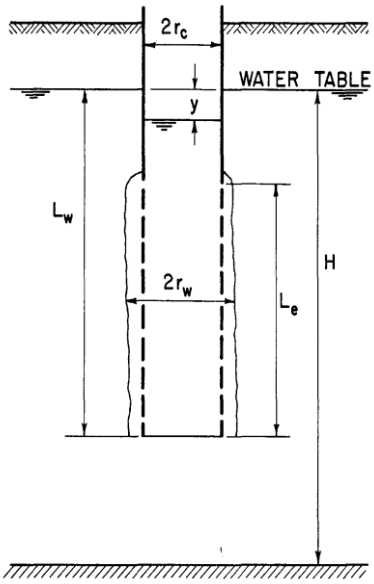

Figure 2-14 Diagram for the Bower and Rice Slug test.

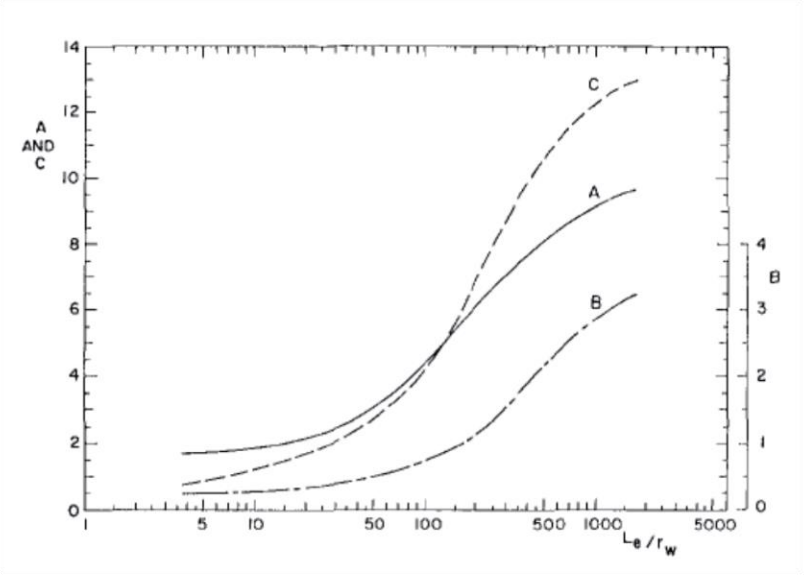

Figure 2-15 Dimensionless parameters for the Bower and Rice Slug test equation (Bouwer 1989).

2.2.4 Bulk Density (BD)

Dry bulk density is the dry weight of soil per given unit of volume and can provide insight into the porosity of the soil or substrate. Due to being unable to drop the water level lower than the substrate level at Hartshorne, a bulk density examination was performed at a single location. At C3S, it was possible to perform three bulk density tests, but the water level was too high in the southwest corner of the cell to perform the bulk density test. At RO and C3N, four bulk density tests were performed.

The bulk density of the substrate was determined based upon the Sand Funnel Method (Method 12-3.2) in Methods of Soils Analysis (Blake and Hartge 1986). Once the water level with each cell was dropped below the surface of the substrate, the vegetative growth and any accumulated sludge was removed and the template for the sand-funnel apparatus was placed on the surface of the organic substrate (Figure 2-16). Through a hole in the template, some of the substrate was removed with a large spoon. The excavated substrate was retained for drying at the laboratory. Once the sample was excavated, the void was filled with a measured volume of sand of known density. In the laboratory, the sample of the substrate was dried to remove the moisture and weighed. The bulk density was calculated with the following equations.

The bulk density (ρ_d) was calculated using the following equation:

$$\rho_d = \frac{dried\ sample\ weight}{volume\ of\ soil} \quad \text{(eq. 2-4)}$$

The volume of sample was calculated using the following equation:

$$volume\ of\ soil = \frac{weight\ sand\ used}{sand\ density} \quad \text{(eq. 2-5)}$$

Figure 2-16 Sand-funnel apparatuses for the Method 12-3.

2.3 Laboratory Methods

2.3.1 Laboratory Falling Head Permeability Tests (L-FHT)

Collected samples were utilized for laboratory-scale falling head permeability tests. The method of Klute and Dirkson (1986) (Method 28-4.2), was followed. A 10.2- mm x 90-mm drain-waste-vent (DWV) PVC drain pipe (standpipe) was spun into the cores collected from the infiltrometer tests. The standpipe was then removed along with substrate within it (Figure 2-17, A).

Once the outside of the pipe was cleaned, a layer of petroleum jelly was liberally applied to the outside bottom of the pipe. The petroleum jelly helped create a water tight seal and lubricated the connection between the standpipe and the base. The standpipe (i.e., pipe and substrate) was placed on a base of layered (B) geotextile, pea gravel (~ 1 cm diameter), and egg sized gravel (~3-5 cm diameter). The housing for the base consisted of a 10.2-cm coupling, 10.2-cm x 10-cm PVC drain pipe and a 10.2-cm PVC cap. In the base

of the cap, a 1.27-cm hole was drilled and tapped for a 1.91-cm threaded PVC 90° elbow (C). A rubber stopper was used to control the flow of water out of the permeameter.

With the apparatus assembled, water was added to fill the standpipe. The water used in these experiments was collected from the respective VFBRs. A pressure transducer was installed within the standpipe to measure the water levels during the test. Once the pressure transducer collected sufficient background information to determine the maximum height

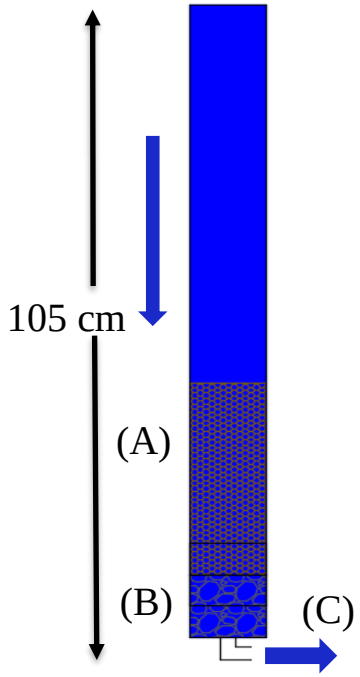

Figure 2-17 An example of the apparatus used for the falling head permeability test.

of the water within the standpipe, the test was started and the rubber stopper removed. The test ran for 30 or 60 minutes, depending on the rate of falling hydraulic head. The rate in the drop of hydraulic head within the standpipe was used to calculate the hydraulic conductivity of the substrate based on Equation 2-1.

2.3.2 Particle Density (PD)

Particle density was used to determine the dry bulk density of samples. Due to the presence of limestone gravel in the treatment media of the Red Oak PTS, only the organic portion of the treatment media was tested. Since the organic substrate would have a density less than 1 g/cm^3, the particle density of the substrate was determined by following the method of Weindorf and Wittie (2003). A 50-g sample of the organic substrate was dried at 70°C for 48 hours to remove moisture. The dried samples were lightly ground to break up the larger organic masses. Once the sample was ground, 10-20 g were placed in a graduated cylinder and weighed. Hexane was then added to the tared graduated cylinder and swirled to displace the gases in the organic substrate. Additional hexane was added to the graduated cylinder to 100 mL and reweighed to determine the total mass of hexane and substrate. Particle density was calculated as follows:

$$\rho_p = \rho_h(W_c)/[\,W_c - (W_{ch} - W_h)] \qquad \text{(eq. 2-6)}$$

where:

ρ_p= particle density (g/cm^3)

ρ_h= density of hexane (g/cm^3)

W_c= weight of oven dried compost (g)

W_{ch}= weight of sample and hexane (g)

W_h= weight of 100 mL pure hexane (g)

2.3.3 Moisture Content (MC)

Moisture content of the substrate was determined by following Garden (1986). The samples from the field bulk density test were weighed (to the nearest 0.1 g) in an aluminum

dish. The samples were then dried at 100-110ºC until constant mass. The samples were then placed in a desiccator until cool. The samples were reweighed to determine the moisture content by difference. The moisture content was calculated using the following equation:

$$\theta_g = \frac{m-d}{d} \quad \text{(eq. 2-7)}$$

Where

θ_g= gravimetric moisture content

m= moist soil mass (g)

d= dry soil mass (g)

2.3.4 Loss on Ignition (LOI)

Loss on ignition estimates the portion of the substrate sample that represents organic matter. Due to the presence of limestone gravel in the treatment media of the Red Oak PTS, only the organic portion of the treatment media was tested. The fraction of soil organic matter (SOM) was estimated by loss on ignition (LOI) following Method 13.2 in Methods of Soil Analysis (Nelson and Sommers 1996). The dried moisture content samples were placed in a muffle furnace at 400ºC for 16 hours. The samples were placed in a desiccator until cool. Once, cool the samples were reweighed to determine the SOM by difference in weight before and after combustion.

The LOI was calculated using the following equation:

$$LOI = \frac{Weight_{105} - Weight_{400}}{Weight_{105}} * 100 \quad \text{(eq. 2-8)}$$

Where:

$Weight_{105}$ = weight of the sample dried at 105°C for 24 hours

$Weight_{400}$= weight of the sample dried at 400°C for 16 hours

2.3.5 Particle Size Analysis

Particle size analyses determines the size distribution of different particle sizes in the substrate sample. Particle size analyses were completed utilizing the Hydrometer Method (Method 15-5) in Methods of Soil Analysis (Gee and Bauder 1986). Samples were dried, crushed and passed through a 200-mesh sieve. Of the portion that passed the 200-mesh screen, 40.0 grams of sample were allowed to soak overnight night in 250 mL DI water and 100 mL of sodium hexametaphosphate solution (50 g/L). The soaked sample was transferred to a metal dispersing cup and mixed with a malted-milk-mixer for 5 minutes.

The suspension was transferred to a sedimentation cylinder and DI water was added to bring the volume to 1 L. A rubber stopper was used to shake the sedimentation cylinder for one minute. After one minute of shaking, the rubber stopper was removed and the hydrometer was lowered into the suspension. Hydrometer readings were taken at 30 seconds and 1 minute. The hydrometer was then removed and dried. At 3, 10, 30, 60, 90, 120 and 1440 minutes the hydrometer was read. Before each reading a blank measurement was taken.

2.4 Summary of Methods

Several different methods were used in the field and laboratory to determine the hydraulic conductivity and characteristics of the organic substrate used in the studied VFBRs. A summary of the methods is shown in Table 2-4.

Table 2-4 Summary of the methodologies.

Test	Parameter measured	Justification
Falling Head Permeability – Field	K	method comparison
Falling Head Permeability – Laboratory	K	method comparison
Modified Single Ring Infiltrometer Test	K	method comparison, sample collection
Slug Test	K	method comparison
Bulk Density	ρ_b	phys. of org. sub., sample collection
Particle Density	ρ_p	phys. characterization of org. sub.
Loss on Ignition	SOM	chem. characterization of org. sub.
Particle Size Analysis - Hydrometer Method	particle size distribution	phys. characterization of org. sub.

Notes: K = hydraulic conductivity, SOM = soil organic matter, phys. = physical, org.= organic, chem. = chemical, sub. = substrate

3 Results and Discussion

3.1 Treatment Media Characterization

3.1.1 Particle Size Analysis

Particle size analyses were completed on the treatment media samples. Table 3-1 shows the fraction that passed 2000-μm screen and photos of the fractions are shown in Figure 3-1. For Red Oak PTS, 85.8% by mass of the material did not pass the screen; therefore, most the treatment media was limestone gravel, which is apparent in the photo (Figure 3-1, bottom-left). C3N and C3S had a similar proportion pass through a 2000-μm screen (~50%), while Hartshorne had much more of the sample pass through the screen. For C3S and C3N most the retained material was wood chips and limestone sand.

Figure 3-2 is a particle size distribution curve for the less than 2000-μm particle size for each cell. Red Oak, C3N and C3S follow a similar curve, however, for Hartshorne

most the sample was in the sand size fraction. Hartshorne had a higher than expected proportion in the sand fraction.

Table 3-1 Weight and percentage of material that passed a 2000 µm screen.

	Total weight	>2000 µm		<2000 µm	
Location	(g)	(g)	(%)	(g)	(%)
RO	874.6	750.6	85.8%	124.0	14.2%
C3N	302.2	151.3	50.1%	150.9	49.9%
C3S	353.9	188.5	53.3%	165.4	46.7%
H	213.7	69.8	32.7%	143.9	67.3%

Figure 3-1 Photos of the greater than 2000 µm fraction (left in each photo) and the less than 2000 µm fraction (right in each photo). The less than 2000 µm fraction was used for the hydrometer test. Top row from left to right C3N, C3S. Bottom row from left to right RO, H.

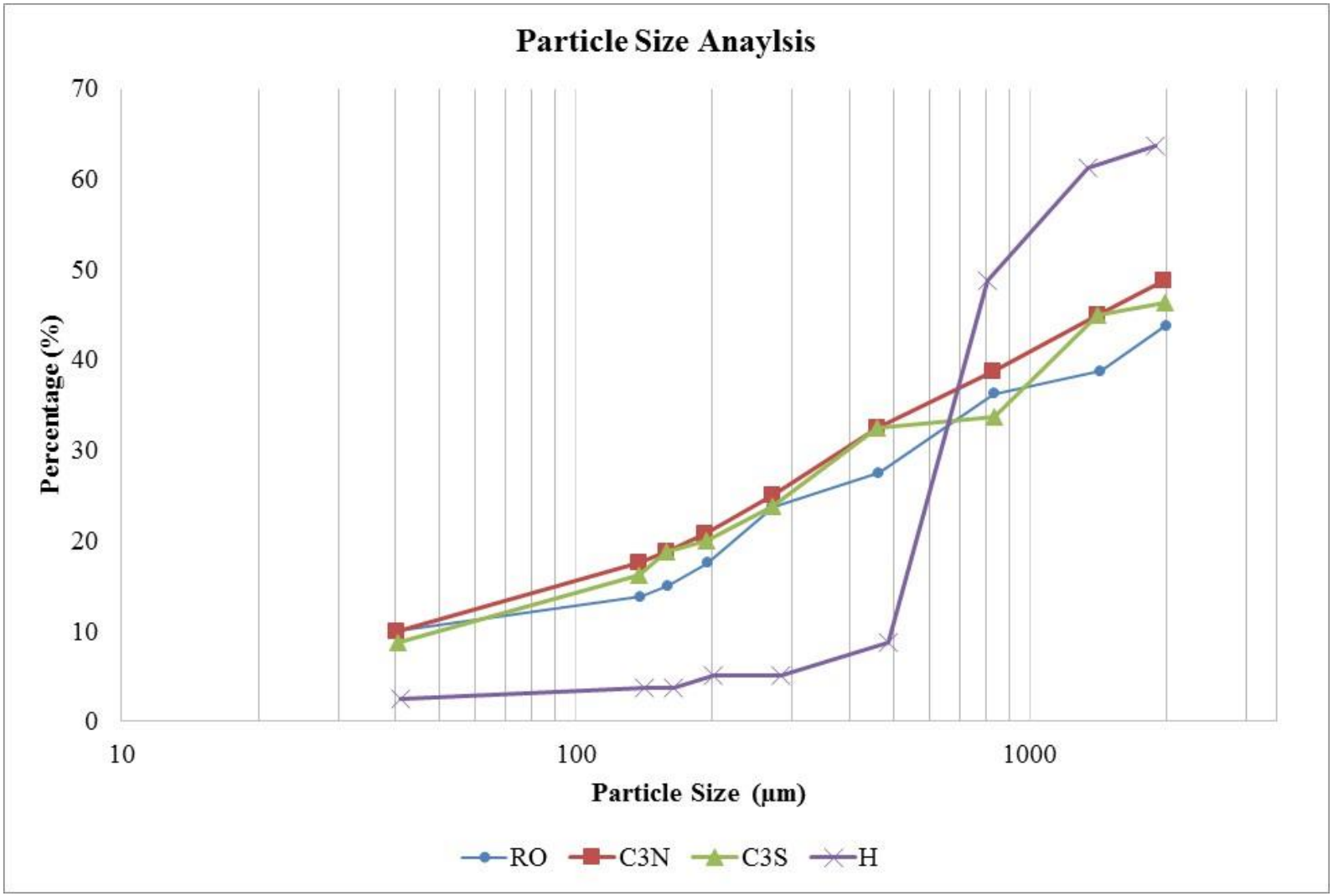

Figure 3-2 Particle size analysis for the smaller than 2000 µm fraction for each VFBR.

3.1.2 Particle Density

The results for particle density are shown in Table 3-2. Statistical differences between means at locations within a given site and between sites were calculated using Student's t-tests (Table 3-3). For each location within a cell, the results were not statistically different. Red Oak PTS was statistically different from all of the other sites, most likely due to the particle density only being performed on the organic treatment media fraction. However, across the sites there were only two locations that were statistically similar, C3N/C3S and C3S/H.

Table 3-2 Particle density measurements for the selected sites.

Location	ρ_p (g/cm^3)	mean (g/cm^3)	s (g/cm^3)
RO - 3	2.0271	1.9329	0.0848
	1.9094	-	-
	1.8624	-	-
RO - 4	1.8879	1.8863	0.1007
	1.9863	-	-
	1.7849	-	-
C3S - 1	2.5868	2.3573	0.2237
	2.1399	-	-
	2.3455	-	-
C3S - 4	2.8327	2.6134	0.3607
	2.8103	-	-
	2.1972	-	-
C3SN- 1	2.5802	2.5896	0.0489
	2.6426	-	-
	2.5462	-	-
C3SN- 3	2.5213	2.3579	0.2746
	2.5116	-	-
	2.0409	-	-
H - 1	2.2872	2.1637	0.1357
	2.1855	-	-
	2.0184	-	-
H- 4	2.1556	2.1901	0.0516
	2.1654	-	-
	2.2495	-	-

Table 3-3 Student's-t test comparison between locations and across different sites. Bolded values are considered statistically different.

Location	Probability
RO 3 and 4	0.559
C3S 1 and 4	0.366
C34 1 and 3	0.280
H 1 and 4	0.776
RO and C3S	**0.005**
RO and C3N	**0.001**
RO and H	**0.0004**
C3S and C3N	0.305
C3S and H	0.055
C3N and H	**0.019**

3.1.3 Bulk Density and Moisture Content

The characterization of the treatment media included determination of the moisture content and bulk density. The results from those tests and a summary of the results are presented in Table 3-4. The measured moisture content of the treatment media may not be representative of the moisture content of the treatment media during operation. That is due to taking the sample while the VFBR was drained. The bulk density of the treatment media varied between each PTS, which is likely due to the composition of the treatment media. The bulk density measurements ranged from 0.25 to 1.10 g/cm^3, with the systems with more organic material having smaller bulk densities.

Table 3-5 is summary of statistical comparisons of moisture content and dry bulk density between sites. Hartshorne PTS could not be included in the Student's t-test since only one sample was taken at that location. Red Oak PTS was statistically different from both C3N and C3S. C3N and C3S were not statistically different for bulk density and moisture content.

Table 3-4 Moisture content and bulk density for each location at each site.

Location	Moisture Content (w)	ρ_d (g/cm^3)	mean (g/cm^3)	s (g/cm^3)
H-1	3.96	0.25	-	-
C3S-1	1.12	0.60	0.51	0.11
C3S-2	1.37	0.52	-	-
C3S-3	1.56	0.39	-	-
C3N-1	1.75	0.40	0.42	0.10
C3N-2	2.23	0.29	-	-
C3N-3	1.57	0.48	-	-
C3N-4	1.23	0.52	-	-
RO-1	0.47	1.00	0.98	0.12
RO-2	0.14	1.10	-	-
RO-3	0.36	1.00	-	-
RO-4	0.51	0.82	-	-

Table 3-5 Student's t test comparisons of moisture content and densities between sites. Bolded values are considered statistically different.

	Probability	
Location	Moisture Content	ρ_d
RO and C3S	**0.004**	**0.003**
RO and C3N	**0.004**	**0.0004**
C3S and C3N	0.220	0.341

3.1.4 Loss on Ignition

To estimate the organic matter in the treatment media samples, loss on ignition (LOI) tests were performed on the collected bulk density samples. The results from the LOI tests and a summary of the results are shown in Table 3-6. Since only one bulk density sample was taken at Hartshorne PTS, LOI was repeated three times on the same bulk density sample. At the other locations, LOI was performed on individual bulk density samples. For the Red Oak PTS samples, the cobbles and gravel were not included in the LOI tests.

Both VFBRs at Mayer Ranch PTS had the lowest LOI of the four sites, and the sample from Hartshorne had the highest LOI. Hartshorne would be expected to have the highest organic carbon content since limestone sand, gravel or cobbles were not added to the treatment media mixture.

Table 3-7 is a summary of statistical comparisons of LOI measurements between sites. As expected, C3N and C3S were not statistically different. Red Oak PTS was not statistically different from C3N and Hartshorne, but not from C3S. Although Hartshorne was statistically different from C3N and C3S, it was not different from Red Oak PTS.

Table 3-6 LOI measurements based upon bulk density samples.

Location	LOI (%)	Average (%)	s (%)
H-1	41.012	41.770	1.782
H-2	43.806	-	-
H-3	40.492	25.898	4.144
C3S-1	24.949	-	-
C3S-2	22.310	-	-
C3S-3	30.434	-	-
C3N-1	32.360	29.755	2.787
C3N-2	31.853	-	-
C3N-3	28.130	-	-
C3N-4	26.677	-	-
RO-1	29.803	35.873	5.130
RO-2	33.540	-	-
RO-3	40.892	-	-
RO-4	39.259	-	-

Table 3-7 Student's t test comparisons of LOI between sites. Bolded values are considered statistically different.

Location	Probability
RO and C3S	**0.037**
RO and C3N	0.095
RO and H	0.102
C3S and C3N	0.249
C3S and RO	**0.012**
C3N and RO	**0.001**

3.2 Hydraulic Conductivity

By comparing multiple methods that examine VFBRs as a whole and as their individual layers, it is possible to estimate hydraulic conductivity for those process units and layers. For this study, 134 separate hydraulic conductivity estimates were completed using four different methods: field falling head, laboratory falling head, slug, and modified single ring infiltrometer tests. The methods can be compared in two different ways: a comparison of a single method across all sites and comparison of all methods at an individual site.

3.2.1 Comparison of Methods Across Multiple Sites

3.2.1.1 Field Falling Head Tests (F-FHT)

F-FHTs were completed at all four VFBRs. With respect to the whole process unit, the field falling head tests are likely the most comparable measurement. The test takes into account the entire system, including the organic treatment media, collection system and effluent control structure. The F-FHTs are also the most representative of operational conditions, due to the low impact and holistic nature of the test. Therefore, the field falling head method will be considered the baseline and used against which to compare other methods.

However, this method is limited in several ways. The method does not identify which layer of the VFBR is the hydraulically constricting layer. Identification of the restrictive layer is necessary when trying to identify the correct rehabilitation method. Additionally, the duration of the tests (up to two weeks) means that repeating the test can take a great deal of time (e.g., months). To repeat the test, the VFBR would have to reach a similar water level elevation as the first test, which could take additional weeks before

the test could begin. The ability to quickly drain the VFBRs is included in the design of the system to help "flush" the system with the intention to improve the hydraulic conductivity. If the system is repeatedly flushed, the hydraulic conductivity could change as a result of the flushing.

It is important to understand these limitations when reviewing these data, but the F-FHT is the only method in this study that takes the whole system into account. Table 3-8 shows the calculated hydraulic conductivities at each of the VFBRs. Due to the tests only being completed once for each cell, a Student's t-test could not be completed for comparisons.

Table 3-8 Contributing Variables and Hydraulic Conductivities for the F-FHT Calculations at each VFBR.

Location	a (cm^2)	L (cm)	A (cm^2)	h_0 (cm)	h_1 (cm)	t (seconds)	K (cm/s)	Log(K)
C3N	1.18E+07	37.49	6.04E+06	83.12	47.31	278100	1.49E-04	-3.83
C3S	1.19E+07	29.26	5.56E+06	41.44	17.71	139500	3.83E-04	-3.42
RO	4.55E+06	91.44	3.88E+06	62.18	28.87	16200	5.07E-03	-2.29
H	7.19E+06	34.5	2.02E+06	43.99	10.79	172800	9.98E-04	-3.00

The calculated hydraulic conductivities are comparable to those measured in other studies. Previously mentioned studies measured the hydraulic conductivity of the newly built Bowden Close and Tan y Garn PTS and found them to range from $6x10^{-3}$ to $3x10^{-3}$ cm/s (Watson et al. 2008; Diaz-Goebes and Younger 2004). For systems that have been in place for more than two years, the hydraulic conductivity decreased from $2x10^{-4}$ to $4x10^{-4}$ cm/s (Watson et al. 2008; Wolkersdorfer et al. 2005). Hydraulic conductivity for all of the VFBRs examined in this study was between 10^{-3} to 10^{-4} cm/s.

Based on this method, the hydraulic conductivity for C4 at Red Oak PTS was the greatest. This VFBR has not been observed to have hydraulic conductivity issues (i.e., water overtopping the berms), which indicates the hydraulic conductivity of the treatment

media was high enough to convey the flow of water entering the cell (although the other VFBR at Red Oak PTS has demonstrated hydraulic conductivity problems). The other three VFBRS have been observed to have hydraulic conductivity issues and have lower measured values than Red Oak PTS.

At the Mayer Ranch PTS, the measured values of C3N and C3S were similar, which may be expected considering the cells are composed of the same material, in the same configurations and have been operational for the same duration of time. However, due to an uncontrolled leaking valve during testing (unknown due to initially elevated water levels), an adjustment to the C3N measurement may be necessary.

At the beginning of the F-FHT for C3N, the inlet pipe to the system was underwater. After the inlet valve was shut, the inlet was manually checked to see if water was entering the cell and no flow was observed. However, two weeks into the test, the inlet was exposed and water could be seen leaking through the valve. Flow was taken at that time and was measured to be 0.54 LPM. Since the calculations for the hydraulic conductivity were made when the inlet was either fully or partially submerged, it is difficult to know the exact impact of the leaking valve, but if the measured flow rate is used as a maximum contribution during testing we can recalculate the hydraulic conductivity based on the HLR. When including the maximum possible flow from the leaking valve the new calculated hydraulic conductivity is 2.02×10^{-4} cm/s.

The Hartshorne VFBR is the oldest system tested, and potentially had the most degraded treatment media of all sites. The VFBR at Hartshorne PTS has been observed to have hydraulic conductivity issues for at least two years prior to testing. The quantity of water passing through the treatment media at Hartshorne PTS had decreased over the years

to 1.9 LPM (measured 2/11/16) with the rest of the water over topping the berms. Water was bypassing the cell and could be assumed to not be getting the designed treatment (e.g., Denholm 2010). The hydraulic conductivity for the Hartshorne PTS VFBR was lower than that of the VFBR at Red Oak PTS, but greater than either cell at Mayer Ranch PTS. Given the age of the system, degree of degradation, and field observations, it was expected Hartshorne would have the lowest hydraulic conductivity. However, those observations do not take into account the hydraulic throughput. The surface area of the treatment media in VFBRs at the Hartshorne PTS VFBR is less than the surface area at Mayer Ranch PTS VFBRs. Therefore, the hydraulic conductivity in the Hartshorne PTS VFBR may have been greater, but the hydraulic throughput was greater at Mayer Ranch PTS VFBRs. That is why operation and maintenance issues were at the Hartshorne PTS VFBR before the other systems.

3.2.1.2 Modified Single Ring Infiltrometer

Since this was a new tool, no methodologies were available and field testing was required to determine the exact technique. In the original design for the MI, no additional weights were included. However, when the standpipe was filled with water the entire MI would lift out of the treatment media. That was due to the 156-cm of head pressure within the system and the 25.4-cm^2 plate on the top of the MI. Based on those numbers, the theoretical weight exerted upwards on the MI was about 79 kg. Olympic barbell weights were added to the top of the MI to counter the head pressure and keep it from moving upward during testing. Figure 3-3 shows the MI in operation with the weights.

Two other issues impacted the funtionality of the MI: water level within the cells during operation and the manometer. The orginal intent of this technique was to draw down

the water level below the surface of the treatment media. However, at all of the sites it took longer to drain and/or pump down the cells than orginally thought therefore, the infiltrometer tests were started when the water level in the cells were less than 15 cm above the top of the treatment media. The infiltrometer was driven into the substrate until the top of the infiltrometer was at the same elevation as the water or the MI reached the bedding material of the drain system. Figure 3-3 shows that there is still standing water on the top of the treatment media during the test.

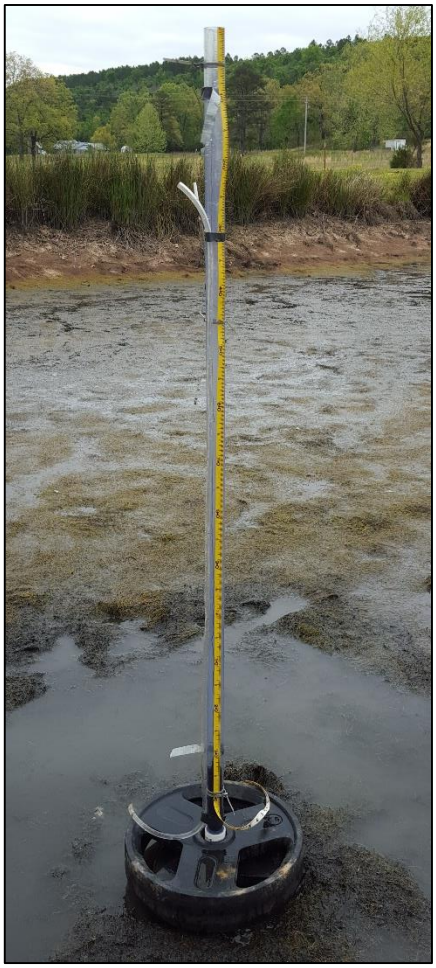

Figure 3-3 Modified single ring infiltrometer in operation at Red Oak PTS.

The manometer proved to be problematic. The manometer was installed for each test, but the readings for each manometer varied dramatically, by up to one meter, between

tests and locations, even within a given VFBR. The problem with getting consistent results were due to either shortcircuiting or plugging. However, it was not possible to know if there were impacts of shortcurcuiting or plugging unless discrepancies were large.

The manometer was intended to measure the head pressure at the bottom of the infiltrometer when water levels were below the surface of the treatment media. However, since the testing was completed with water still on the surface of the treatment media, it is possible to use the measurement of the water level on the outside of the infiltrometer. Using the water level in the cell elminated the inconsistancies associated with the manometer and provided more realiable results. At each location the infiltrometer test was conducted three times. Table 3-9 shows the mean values for each infiltrometer location. Table 3-9 represents a total of 51 individual infiltrometer tests.

Table 3-9 Average hydraulic conductivity numbers for the modified infiltrometer at all sites.

Location	K (cm/s)	s (cm/s)	Log(K)
H - 1	3.64E-04	5.92E-06	-3.44
H - 2	3.08E-04	7.16E-06	-3.51
H - 3	3.53E-03	2.68E-04	-2.45
H - 4	9.92E-04	4.11E-04	-3.00
C3N - 1	6.63E-04	1.44E-04	-3.18
C3N - 2	1.01E-04	3.37E-05	-4.00
C3N - 3	5.52E-04	5.15E-06	-3.26
C3N - 4	7.54E-04	2.11E-04	-3.12
C3N - 5 *	8.96E-04	4.41E-05	-3.05
C3S - 1	2.66E-03	9.55E-05	-2.58
C3S - 2	2.65E-03	9.58E-05	-2.58
C3S - 3	9.96E-03	9.01E-04	-2.00
C3S - 4	8.84E-05	4.70E-06	-4.05
RO - 2	2.27E-03	9.79E-05	-2.64
RO - 3	7.12E-04	2.22E-04	-3.15
RO - 4	1.63E-03	8.02E-04	-2.79
RO - 5 *	3.08E-03	2.12E-04	-2.51

Notes: Locations with an * were done with the vegetation removed. The vegetation was not removed at all locations due to the lack of vegetation. n=51.

With the exception of one location (C3S – 4), all of the hydraulic conductivities at each location fall within the range of $9x10^{-3}$ to $1x10^{-}4$ cm/s. Student's t-tests were calculated, with $\alpha=0.05$, and the probabilities are shown in Table 3-10. With the exception of two comparisons, the results indicate that infiltrometer data are not significantly different between each system.

However, the comparisons between C3N and C3S were significantly different ($p < 0.014$). Since those two cells are the most similar, it is expected that they would have similar values. C3N was also significantly different than RO, which makes C3N similar only to the VFBR at Hartshorne.

Table 3-10 Statistical comparison of the infiltrometer data between each site. Bolded values are considered statistically different.

Comparison	Probability
RO vs C3N	**0.001**
RO vs C3S	0.122
RO vs H	0.215
C3N vs C3S	**0.014**
C3N vs H	0.110
C3S vs H	0.051

3.2.1.3 Slug Tests

Slug tests (ST) were completed at the Mayer Ranch and Red Oak PTS (Table 3-11). The testing apparatus at both locations were installed during construction. The differences between the two systems make it difficult for a direct comparison. At Mayer Ranch PTS, horizontal porewater samples were installed and at Red Oak PTS vertical piezometers were installed.

Since the porewater samplers and piezometers were installed at different angles the measured hydraulic conductivities are in different directions. For the Bower and Rice slug test, the measured K is perpendicular to the screened section of the sampler/piezometer.

Since the porewater samplers are horizontal at Mayer Ranch PTS the hydraulic conductivity is measured in the vertical direction and at Red Oak PTS the hydraulic conductivity is measured in the horizontal direction. During normal operation of the VFBRs the direction of flow is in the vertical direction.

Table 3-11 Bower and Rice Slug tests for Red Oak and Mayer Ranch PTS.

Location	Depth (m)	K (cm/s)	s (cm/s)	Log(K)
C3N-N-Blue	0.23	2.22E-04	3.78E-06	-3.65
C3N-N-Yellow	0.23	2.30E-04	1.80E-05	-3.64
C3N-M-Black	0.23	1.71E-04	7.69E-06	-3.77
C3N-M-Blue	0.23	1.98E-04	5.50E-06	-3.70
C3N-M-Yellow	0.23	2.00E-04	4.68E-06	-3.70
C3N-S-Blue	0.23	3.15E-04	3.44E-06	-3.50
C3N-S-Yellow	0.23	2.00E-04	5.48E-06	-3.70
C3S-N-Blue	0.23	2.92E-04	8.43E-07	-3.53
C3S-N-Yellow	0.23	1.98E-04	1.29E-05	-3.70
C3S-M-Black	0.23	2.14E-04	4.21E-06	-3.67
C3S-M-Blue	0.23	1.46E-04	7.63E-06	-3.84
C3S-M-Yellow	0.23	2.50E-04	8.89E-06	-3.60
C3S-S-Blue	0.23	1.56E-04	3.73E-06	-3.81
C3S-S-Yellow	0.23	1.35E-04	6.53E-06	-3.87
RO - 1A	1.0	1.95E-04	-	-3.71
RO - 1B	0.3	2.47E-04	-	-3.61
RO - 2A	1.0	1.71E-04	-	-3.77
RO - 2B	0.3	7.28E-05	-	-4.14
RO - 5A	1.0	1.44E-04	-	-3.84
RO - 5B	0.3	1.25E-04	-	-3.90
RO - 6A	1.0	1.71E-04	-	-3.77
RO - 6B	0.3	2.72E-05	-	-4.57
RO - 9A	1.0	1.74E-05	-	-4.76
RO - 9B	0.3	4.33E-05	-	-4.36

Notes: At Red Oak PTS the nested piezometers were only measured once, therefore a standard deviation could not be calculated. n=52.

No literature values for slug tests measurements for piezometers in VFBRs of PTS were found, but the calculated hydraulic conductivities were comparable to those obtained by tracer studies of VFBRs (Watson et al. 2008; Diaz-Goebes and Younger 2004). A

comparison of slug test values in an organic matrix can be made by looking at Surride et al. (2005). This study focused on slug tests in peatlands and reported values in the range $1x10^{-4}$ to $1.6x10^{-3}$ cm/s, which are within an order of magnitude from the calculated VFBR slug test values (Surride et al. 2005)

At Red Oak PTS (Figure 2-5), nested piezometers were installed in pairs at nine different locations throughout the VFBR. Each pair were set to a depth of 0.3 m and 1.0 m, and five of the nine locations were tested. A Student's t test was performed and showed there was no significant difference between the different depths (p=0.49).

Comparing the methods between the sites showed significant differences between Red Oak and Mayer Ranch. Considering the differences in the ways the porewater samplers and piezometers were installed, and the similarities in the cells at Mayer Ranch, these results may be expected.

Table 3-12 Student t-test comparisons of slug tests for each site. Bolded values are considered statistically different.

Comparison	Probability
RO vs C3N	**0.003**
RO vs C3S	0.014
C3N vs C3S	0.194

3.2.1.4 Laboratory Falling Head Tests

The laboratory falling head tests (L-FHT) were completed for all four VFBRs using the recovered cores from the MI tests. The cores were transported back to the University of Oklahoma campus and tested in the Center for Restoration of Ecosystems and Watersheds (CREW) laboratories. The vibrations from transportation may have impacted the estimated hydraulic conductivity of the treatment media. Another potential source of error is the diameter of the apparatus used for the L-FHT. Since the diameter of the

apparatus for L-FHT is smaller than the MI, the ratio of water passing through the treatment media in relation to the water passing along the contact between the wall of the PVC pipe and the treatment media could impact the results. The names listed in Table 3-13 correspond with the locations for the infiltrometer tests.

Table 3-14 shows the statistical comparison between the sites. This method created higher variability than other methods. This could be related to the relatively small differences between h_o and h_t, which for could be as small as a few centimeters. With the exception of three tests the standard deviation was within the same order of magnitude.

Table 3-13 Hydraulic conductivities for the laboratory falling head tests.

Location	K (cm/s)	s (cm/s)	Log(K)
H - 1	1.79E-03	2.61E-04	-2.75
H - 4	3.22E-04	1.20E-04	-3.49
C3N - 1	8.04E-04	7.72E-05	-3.09
C3N - 3	2.07E-03	7.92E-04	-2.68
C3S - 1	4.01E-04	8.30E-05	-3.40
C3S - 4	5.91E-04	2.12E-05	-3.23
RO - 3	2.70E-04	2.13E-04	-3.57
RO - 3 w/ out veg	6.71E-04	5.59E-04	-3.17
RO - 4	4.76E-03	7.43E-04	-2.32

Notes: Only one location was tested without vegetation due to the other cores not having an appreciable amount of vegetation. n= 27.

Due to the high variability for this method, only one comparison was found to be significantly different (Table 3-14). The significant difference was found between C3N and C3S at Mayer Ranch PTS. That was not expected considering the previously discussed similarities between the cells. This could be due to the transportation of the material from site or the wall effects from apparatus.

Considering the results from the MI tests (Table 3-10), where there was also a significant difference between values for C3N and C3S, the relative differences in

calculated hydraulic conductivities are not the same. For the infiltrometer, C3S had the greater conductivity, while for the L-FHT, C4N had the greater hydraulic conductivity.

Table 3-14 Student t comparisons of laboratory falling head tests for each site. Bolded values are considered statistically different.

Comparison	Probability
RO vs MR C3N	0.580
RO vs MR C3S	0.092
RO vs H	0.317
C3N vs C3S	**0.043**
C3N vs H	0.448
C3S vs H	0.158

3.2.2 Comparison of Sites

Table 3-15 summarizes the means all methods across all sites and will be referenced throughout the following sections. The table include the log of the hydraulic conductivity for easy comparison.

Table 3-15 Summary of methods across all of the selected cells.

		RO	C3N	C3S	H
F-FHT	K (cm/s)	5.07E-03	1.49E-04	3.53E-04	9.98E-04
	s (cm/s)	-	-	-	-
	log(K)	-2.29	-3.83	-3.45	-3.00
MI	K (cm/s)	1.21E-04	2.19E-04	1.99E-04	1.30E-03
	s (cm/s)	7.79E-05	4.46E-05	5.55E-05	1.39E-03
	log(K)	-3.92	-3.66	-3.70	-2.89
L-FHT	K (cm/s)	1.93E-03	5.93E-04	3.84E-03	1.05E-03
	s (cm/s)	9.79E-04	2.97E-04	3.87E-03	8.23E-04
	log(K)	-2.72	-3.23	-2.42	-2.98
ST	K (cm/s)	1.90E-03	1.44E-03	4.96E-04	-
	s (cm/s)	2.21E-03	8.57E-04	1.17E-04	-
	log(K)	-2.72	-2.84	-3.30	-

3.2.2.1 Mayer Ranch PTS - C3N

For the C3N cell of the Mayer Ranch PTS, four different methods were utilized to calculate the hydraulic conductivity: F-FHT, MI, L-FHT, and ST. Figure 2-9 shows the locations of the pore water samplers and MI tests. The locations of MI-3 through MI-5 were slightly north of the intended location within the cell and that was due to the uneven distribution of the treatment media. At the time of testing, the southern end of the cell had excess water, due to difficulties with pumping, precluding performance of the MI tests at the originally intended locations.

Table 3-15 shows the mean hydraulic conductivities measured for each location within C3N and Figure 3-4 graphically represents the data. All of the tests, with exception of one of the L-FHT tests, were within$1x10^{-4}$ to $6x10^{-4}$ cm/s. Like Red Oak, the F-FHT did not fall within the standard deviations of the ST, MI or L-FHT (Table 3-15). However, unlike Red Oak, all the point measurement K values were greater than the F-FHT, with the L-FHT showing the greatest difference. The ST hydraulic conductivity values were much closer to the F-FHT than at Red Oak. However, the F-FHT value did not fall within one standard deviation of the ST since the variability was considerably lower at C3N. One potential reason the ST was closer to the F-FHT test is the way in which the porewater samplers were installed. Instead of a sand pack, the porewater samplers were placed directly in the treatment media, which eliminated any interferences a sand pack may have played.

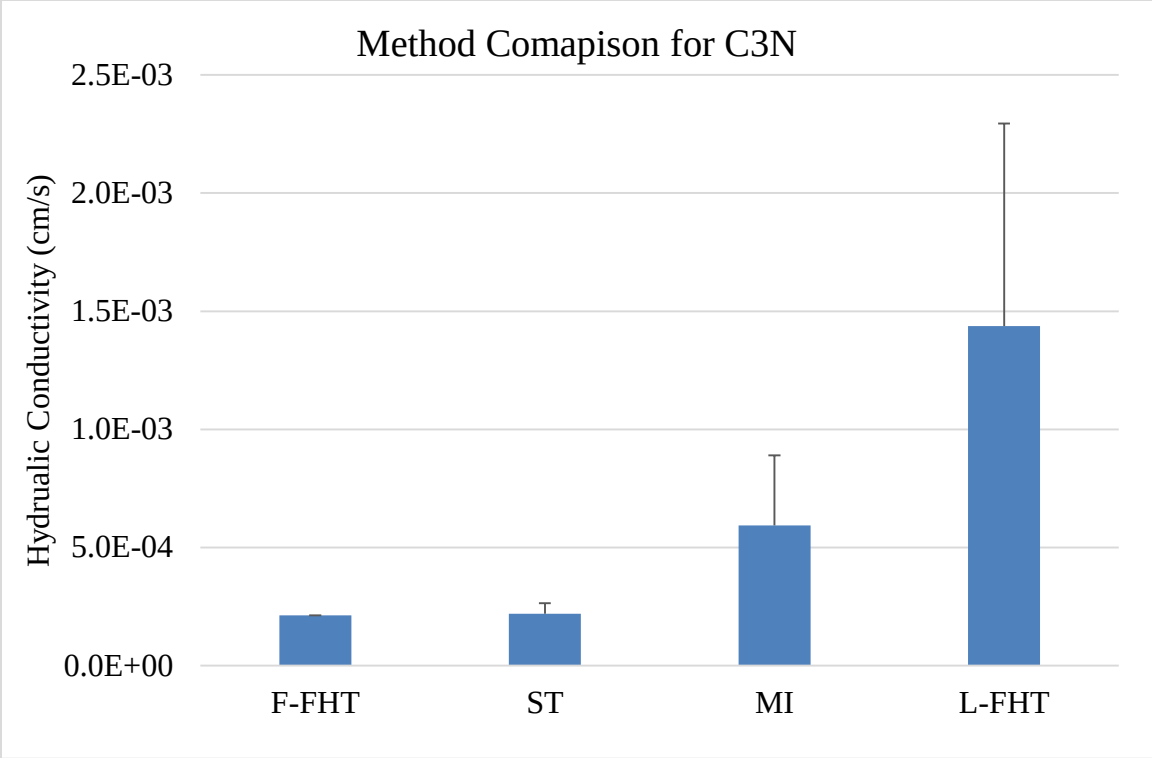

Figure 3-4 Results of four different hydraulic conductivity tests for C3N at Mayer Ranch.

Statistically comparing the methods to each other, L-FHT and MI are the only methods that resulted in a probability value greater than 0.05 (Table 3-16). The statistical comparison results are similar to those at Red Oak PTS.

Table 3-16 Student t-test comparison of point methods at C3N at Mayer Ranch PTS. Bolded values are considered statistically different.

Comparison	Probability
ST vs MI	**0.0002**
ST vs L-FHT	**0.018**
L-FHT vs MI	0.060

3.2.2.2 Mayer Ranch PTS - C3S

For the C3S VFBR of the Mayer Ranch PTS, the same four methods were utilized to calculate hydraulic conductivity. Figure 2-10 shows the locations of the pore water samplers and MI tests. The location MI-4 was slightly north of the intended location due to

the uneven distribution of the treatment media. At the time of testing, the south-western end of the cell had excess water to be able to perform the MI tests. Very little vegetation was present during testing, so an MI test without vegetation was not performed.

Table 3-15 shows the mean hydraulic conductivity measured for each location within C3S and Figure 3-5 graphically represents the data. For each location in Table 3-15, the test was repeated three times, except for F-FHT. All the tests were within $3x10^{-3}$ to $2x10^{-4}$ cm/s. Similar to ST-derived K values at C3N, the variability in the ST values for C3S were relatively small when compared to other methods. For the MI tests, MI-4 was more than an order of magnitude slower than the other locations within the VFBR.

The F-FHT K value does not fall within the standard deviations of the ST, but the F-FHT does fall within one standard deviation for MI and L-FHT (Table 3-15). However, the MI hydraulic conductivity values only encompass the F-FHT when including the MI-4 value (Figure 2-10). When that test is removed from the calculations, the F-FHT no longer falls within one standard deviation. This is important to note because those measurements are nearly an entire order of magnitude different. Table 3-17 statistically compares the different methods using the Student's t-test. For C3S, not one of the methods was statistically similar, even when removing the fourth MI test.

Table 3-17 Student's t-test comparison of point methods at C3S at Mayer Ranch PTS. Bolded values are considered statistically different.

Comparison	Probability
ST vs MI	**0.008**
ST vs L-FHT	**0.001**
L-FHT vs MI	0.012

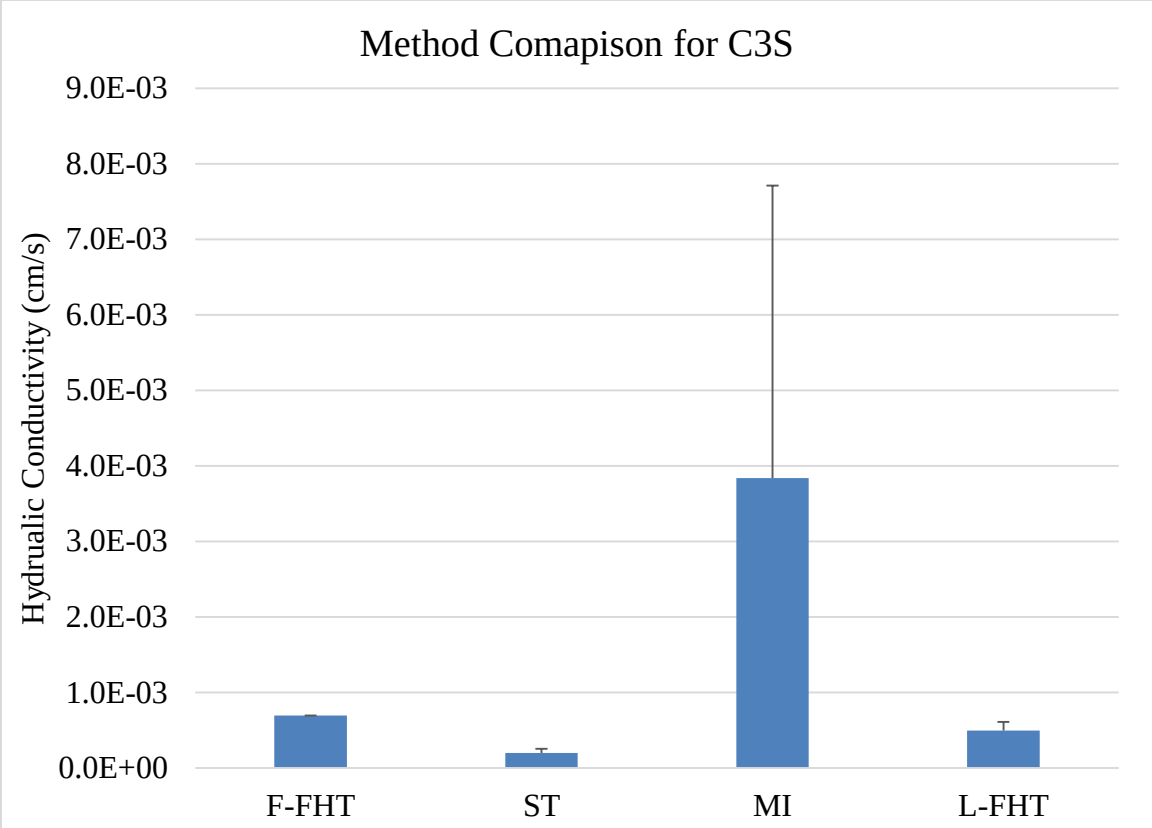

Figure 3-5 Results of four different hydraulic conductivity tests for the C3S at Mayer Ranch PTS.

3.2.2.3 Red Oak PTS

For the Red Oak PTS, four different methods were utilized to calculate the hydraulic conductivity: F-FHT, MI, L-FHT, and ST methods. Figure 2-12 shows the locations of the ST and MI tests. Table 3-15 shows the total mean hydraulic conductivity, if available, for each method measured at Red Oak PTS.

Since the F-FHT hydraulic conductivity was only measured once, the number of statistical tests that could be performed were limited. For comparisons, the F-FHT will be compared to the other tests by examining if the F-FHT K value falls within one standard deviation of the other value. For Red Oak PTS, the F-FHT does not fall within one standard deviation of the ST, MI or L-FHT determined K values. All of the point measurements

(i.e., MI, L-FHT and ST) were smaller than the F-FHT. Figure 3-6 graphically compares the methods at the Red Oak PTS.

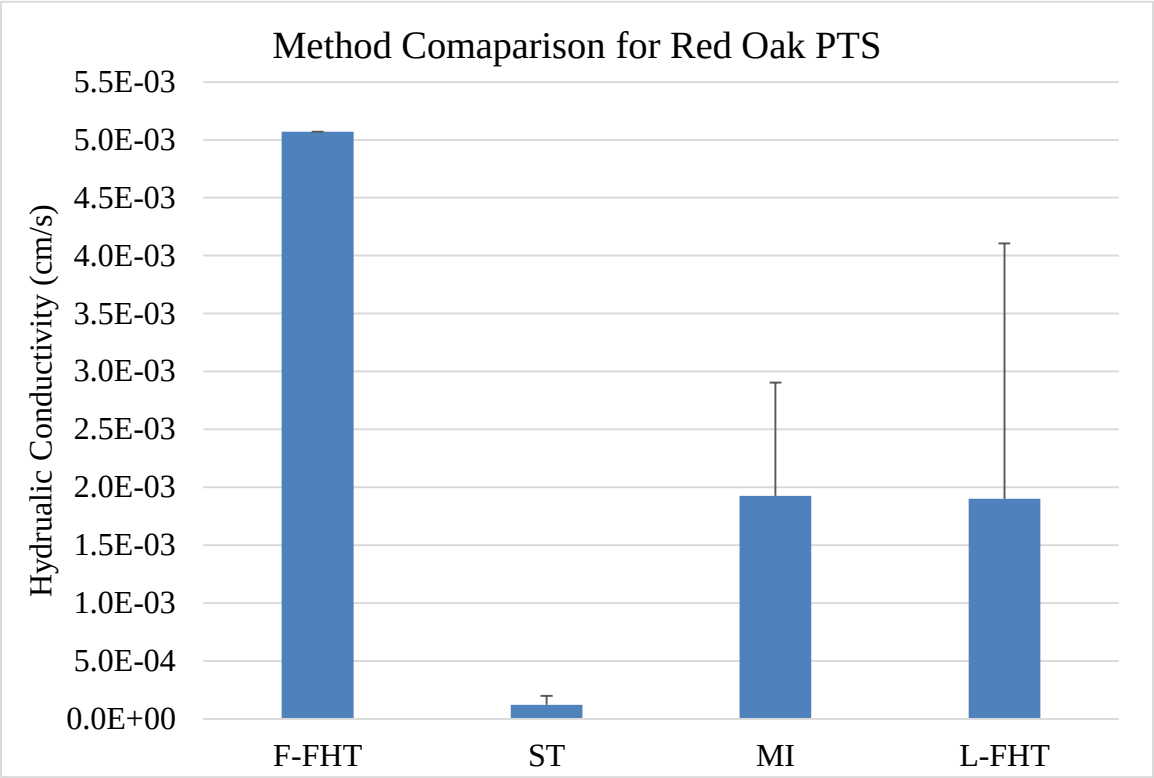

Figure 3-6 Results of four different hydraulic conductivity tests for C4 at Red Oak PTS

The ST method was expected to return similar results to the F-FHT because the piezometers had been in place since construction and would have had little to no disturbance during testing. The difference in measurements could be related to several issues. Since the piezometers were installed vertically, the measured hydraulic conductivity is perpendicular to the flow of water during normal operation. Possibly both measurements were accurate and the treatment media is anisotropic.

Several different issues could have impacted the measurements. Since the piezometers were packed in 15 cm of sand, these tests may be more representative of conditions within the sand pack than in the surrounding treatment media. Preferential

precipitation of metals or biological precipitates may have caused decreased permeability within the sand pack. Additionally, the screened section of the piezometer may have become occluded overtime with precipitates or biological growth. The blockage is most likely due to biological growth, because of the low metal concentration within that unit. Without additional testing of the sand pack or autopsy of the piezometer it is difficult to ascertain the root cause of the differences.

The statistical testing between the F-FHT and the other methods is limited due to the singular measurement for the F-FHT, but it is possible to statistically compare the other methods to each other. Table 3-18 shows the Student's t-tests between each of the point methods at the Red Oak PTS. The ST method was statistically different from the L-FHT and the MI method. Comparing the MI method with the L-FHT shows there is no significant difference between these methods. The L-FHT were cored from the MI cores, therefore it would be expected that the values would be similar.

Table 3-18 Student's t-test comparison of point methods at the Red Oak PTS. Bolded values are considered statistically different.

Comparison	Probability
ST vs MI	**0.001**
ST vs L-FHT	**0.042**
L-FHT vs MI	0.976

3.2.2.4 Hartshorne PTS

For the fourth cell at the Hartshorne PTS, three different methods were utilized to calculate the hydraulic conductivity: F-FHT, MI, and L-FHT. This site did not have previously installed piezometers or porewater samplers to perform ST. Figure 2-7 shows the locations of the MI tests. Very little to no vegetation was present during testing so an MI test without vegetation was not performed.

Table 3-15 is the mean hydraulic conductivity measured for each location within Hartshorne and is graphically shown in Figure 3-7. For each location in Table 3-15, the test was repeated three times, except for F-FHT. All the tests were within $1x10^{-3}$ to $9x10^{-4}$ cm/s. The eastern edge of the cell had lesser hydraulic conductivity by an order of magnitude than the western side.

Unlike the other sites, the F-FHT falls within the standard deviations of the MI and L-FHT (Table 3-15). This is the only site where the MI and the L-FHT K values encompassed the F-FHT K value. Statistically comparing the K values derived from L-FHT and MI with a Student's t-test resulted in a p= 0.648, which indicates that the two data sets are not statistically different.

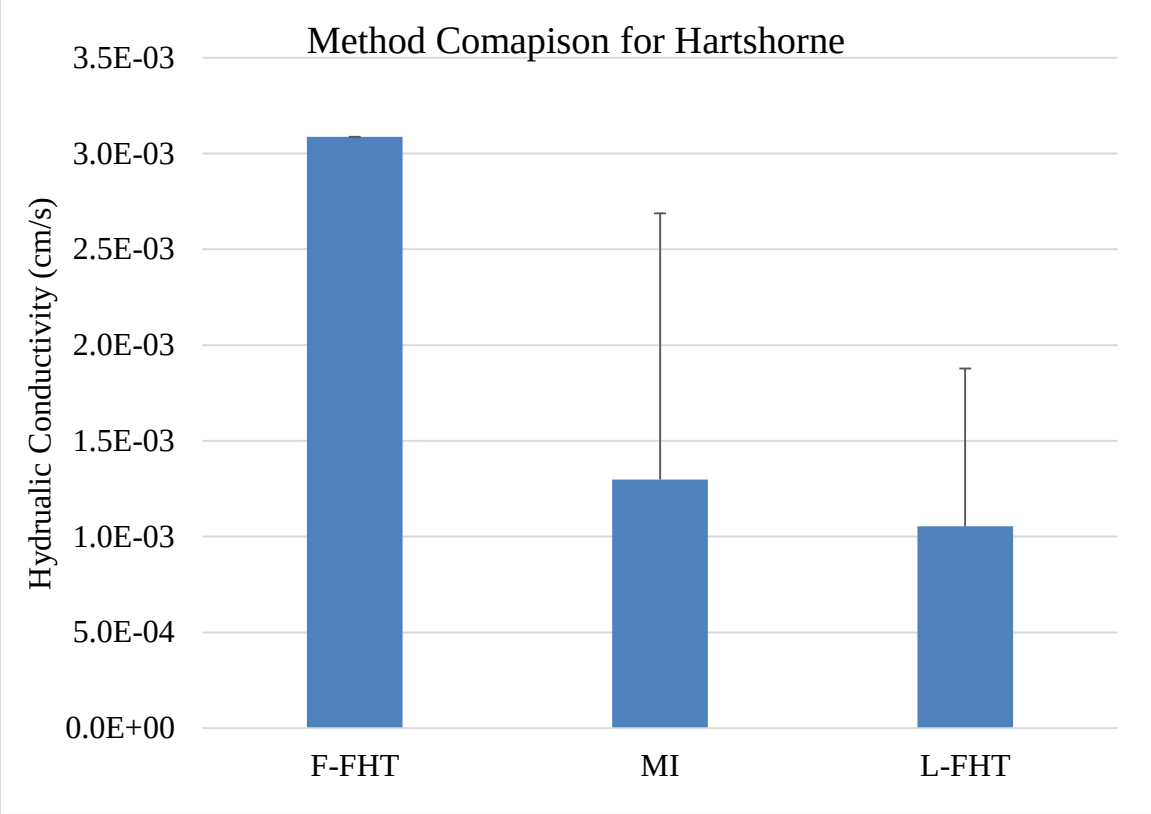

Figure 3-7 Results of four different hydraulic conductivity tests for C4 the Hartshorne PTS.

3.3 Treatment Media vs. Hydraulic Conductivity

A comparison of the treatment media characteristics to the hydraulic conductivity may help illuminate if there are treatment media parameters that could help predict the hydraulic conductivity and vice versa. With the collected data, it is possible to the make a comparison between porosity, bulk density, particle density, moisture content and LOI parameters with the different hydraulic conductivity methods. For the following comparison, the method and parameter were averaged for each cell and then compared across different cells. This method compares one treatment media parameter to multiple hydraulic conductivity measurements. That leads to the hydraulic conductivity data being grouped, but this grouping does not represent any trends. Table 3-19 summarizes the data for each parameter and methods for hydraulic conductivity.

Table 3-19 Summary of the averaged parameters and hydraulic conductivities for each selected cell.

Parameter		RO	H	C3N	C3S
Porosity	mean	0.487	0.888	0.830	0.796
	s	0.185	-	0.0416	0.0569
Particle Density	mean	1.9097	2.1769	2.4738	2.4854
(g/cm^3)	s	0.0871	0.0930	0.2173	0.3028
Bulk Density	mean	0.98	0.25	0.42	0.51
(g/cm3)	s	0.12	-	0.10	0.11
Moisture Content	mean	0.37	3.96	1.70	1.35
(w)	s	0.17	-	0.42	0.22
LOI	mean	35.8734	41.7700	29.7553	25.8979
(%)	s	5.1296	1.7825	2.7868	4.1442
MI K	mean	3.74E-04	1.73E-04	9.85E-05	2.74E-04
(cm/s)	s	3.76E-04	2.01E-04	9.61E-05	4.20E-04
L-FHT K	mean	1.90E-03	1.05E-03	1.44E-03	4.96E-04
(cm/s)	s	2.21E-03	8.23E-04	8.57E-04	1.17E-04
ST K	mean	1.21E-04	-	2.28E-04	2.00E-04
(cm/s)	s	7.79E-05	-	4.86E-05	5.44E-05
F-FHT K	mean	5.07E-03	9.98E-04	1.49E-04	3.83E-04
(cm/s)	s	-	-	-	-

Figure 3-8 shows the comparison between porosity and hydraulic conductivity. For the ST, MI, and L-FHT there do not appear to any trends, however for the F-FHT, a weak trend show that as the porosity increases the hydraulic conductivity trends downward. A linear trend line applied to the data has an R^2 =0.5946. A similar trend was documented by Beard and Weyl (1973). As the grain size becomes finer, the porosity increases, but the hydraulic conductivity decreases (Beard and Weyl 1973). The decrease in hydraulic conductivity is even greater in materials that are poorly sorted (Beard and Weyl 1973), such as mixed treatment media in the VFBRs.

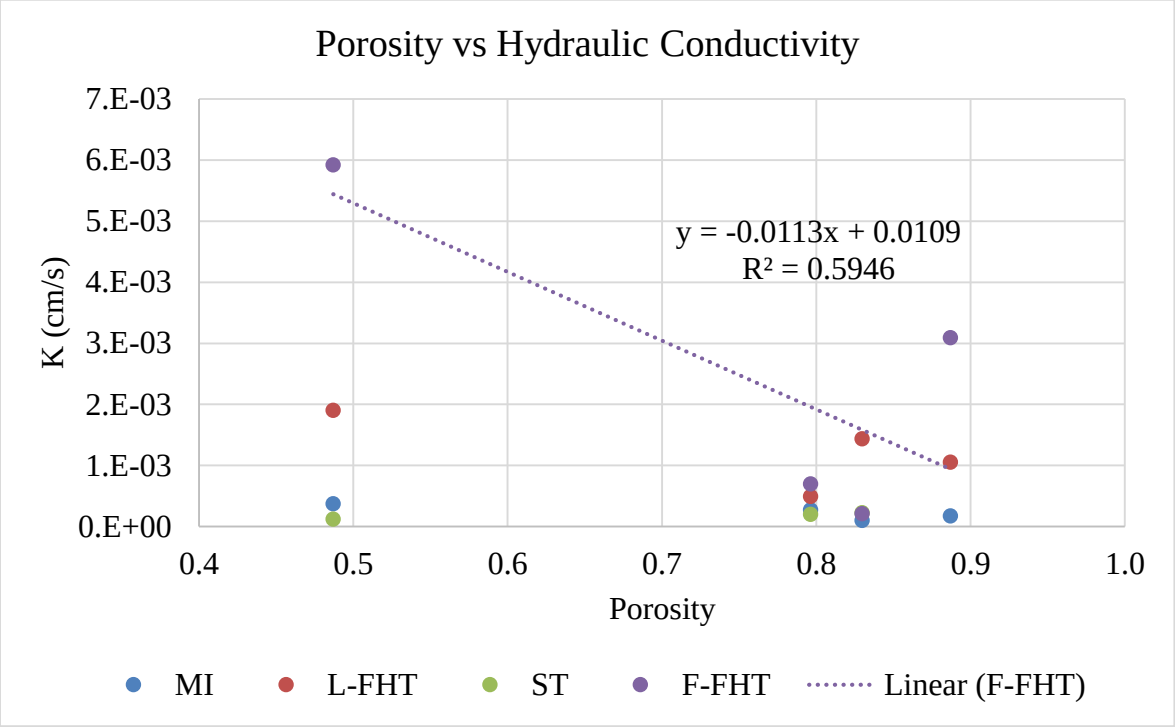

Figure 3-8 Comparison of porosity with hydraulic conductivity across VFBRs.

Figure 3-9 shows the comparison between particle density and hydraulic conductivity. For the ST, MI, and L-FHT there do not appear to any trends, however for the F-FHT, as the particle density increases the hydraulic conductivity trends downward. A linear trend line applied to the data has an R^2 =0.9888. As the density of the particles

increase, the hydraulic conductivity decreases. There has been no indication that particle density is relation to particle density in traditional soils, but one may exist here due to the difference in densities between the organic material and limestone.

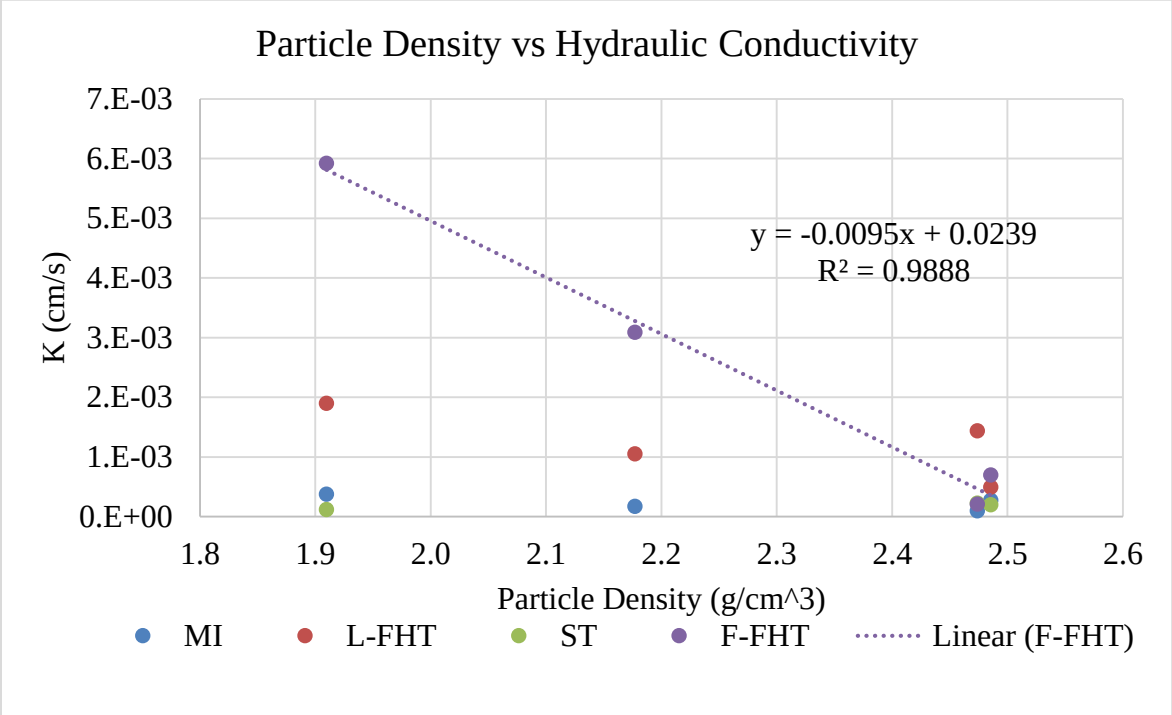

Figure 3-9 Comparison of particle density with hydraulic conductivity across the VFBRs.

The comparison between bulk density and the hydraulic conductivity did not show the same relationship (Figure 3-10). As the bulk density increased, the hydraulic conductivity increased, which is the opposite of the particle density relationship. Considering the close relationship between particle density and bulk density it would be expected that the trends would be similar. Once again, the disparities in the numbers may be related to the different densities of the organic material compared to the density of the limestone.

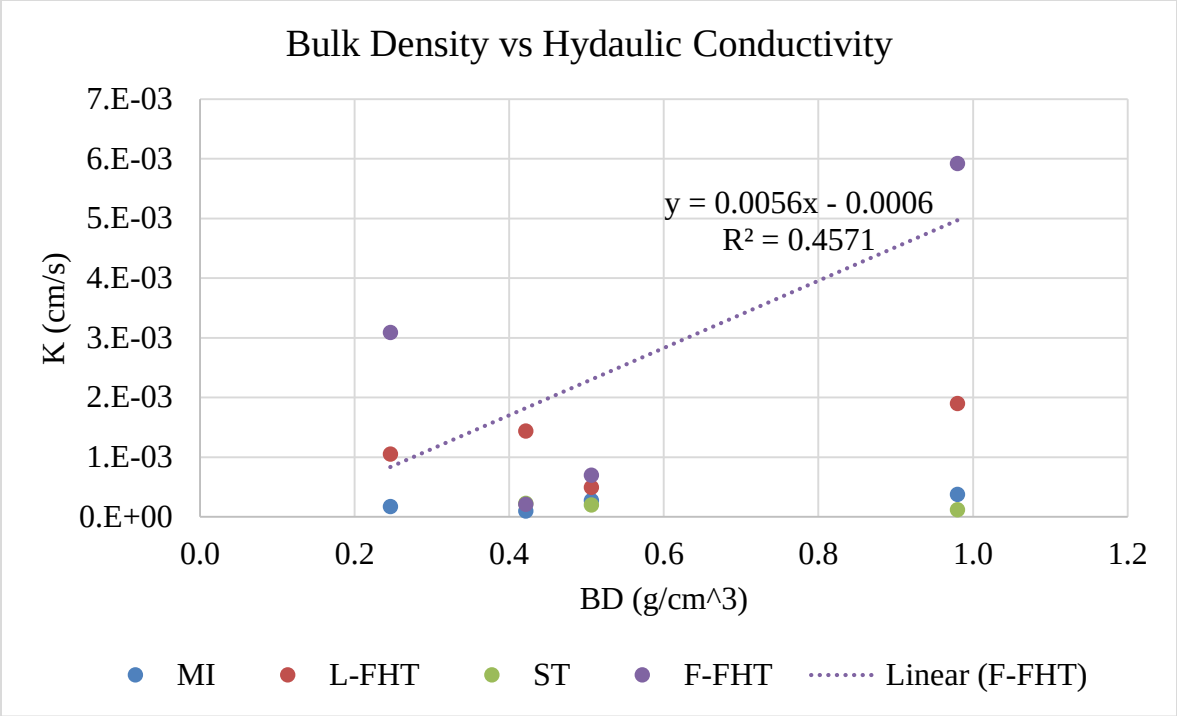

Figure 3-10 Comparison of bulk density with hydraulic conductivity across the VFBRs.

The comparisons between moisture content and LOI also showed weak to no trends (Figure 3-11, Figure 3-12). As the systems age, the organic material is broken down and consumed by sulfate reducing bacteria. As the organic material is consumed, it is likely that the material should become more compact. Therefore, it could be expected that as the LOI decreases, the hydraulic conductivity would decrease. For the F-FHT there is a very weak trend in the LOI to that gives evidence for that claim.

The trend between particle density and hydraulic conductivity is the only strong trend that appears in the comparisons between the treatment substrate characteristics and hydraulic conductivity. The porosity does show a trend with hydraulic conductivity, but the trend is not as strong as particle density trend. Based upon the collected data, bulk density, moisture content, and loss on ignition show weak to no trends related to hydraulic conductivity.

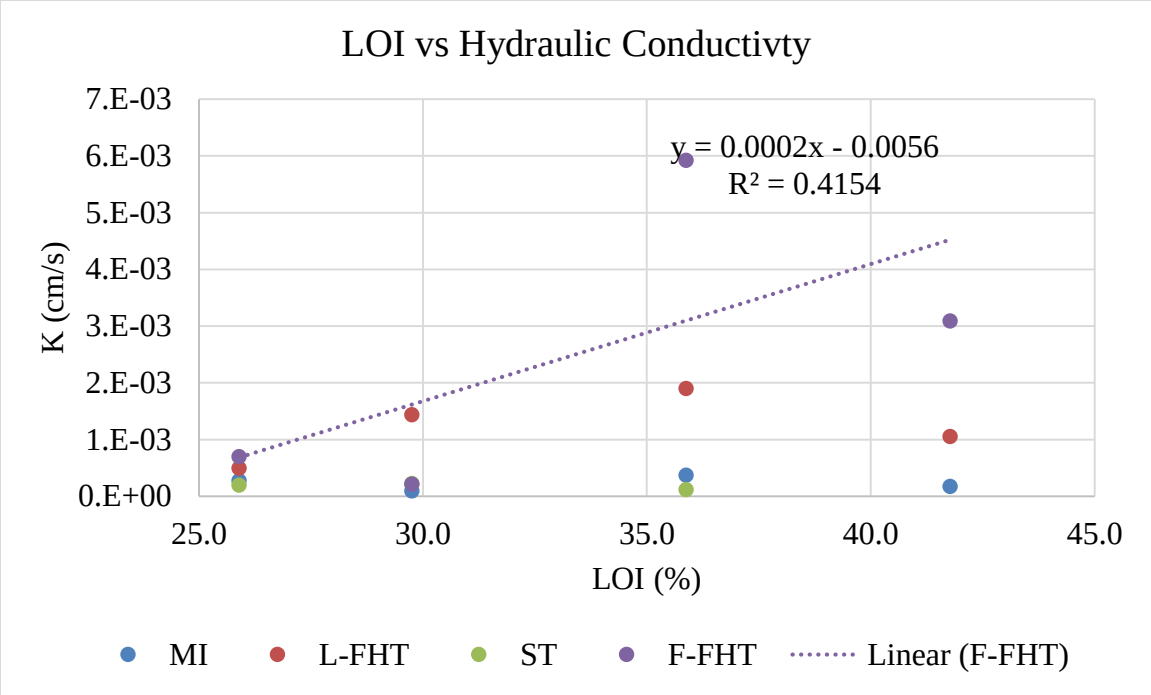

Figure 3-11 Comparison of moisture content with LOI across the VFBRs.

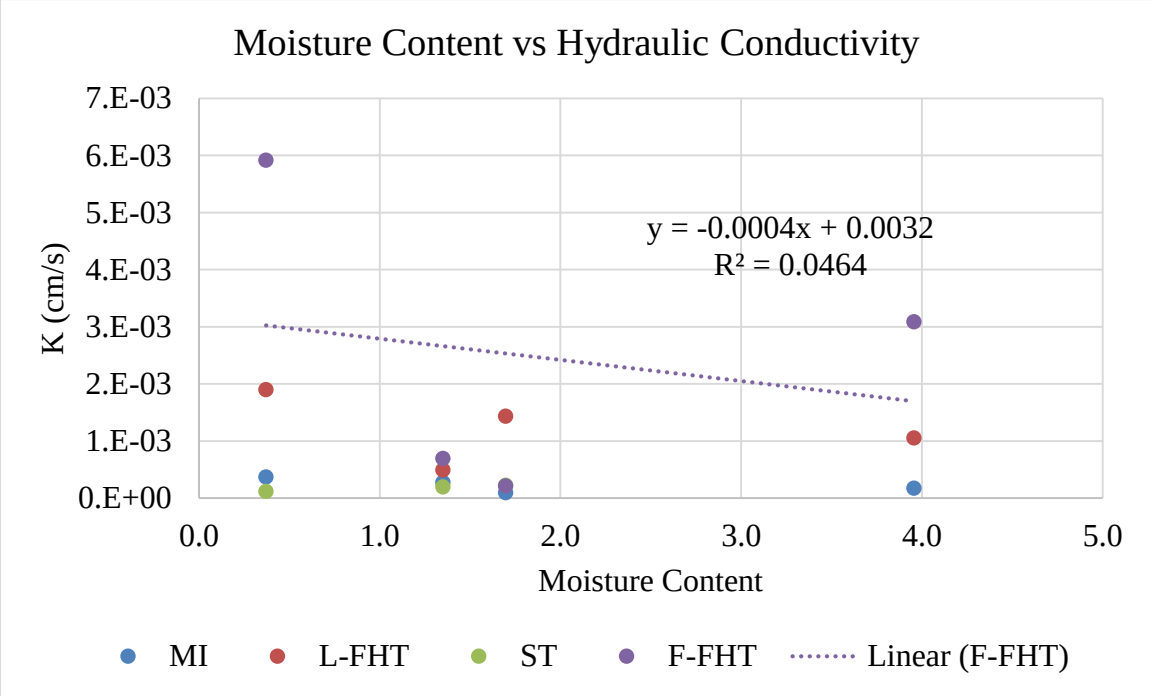

Figure 3-12 Comparison of moisture content with hydraulic conductivity across the VFBRs.

4 Conclusions

A comparison of measurement methods at different VFBRs gave insight into various hydraulic conductivities of the cells. A total of 134 individual hydraulic conductivity tests were completed, utilizing four different methods, to estimate the hydraulic conductivity of the entire VFBR or the treatment media. In addition to the hydraulic conductivity tests, the treatment media were characterized to identify if any parameters could predict hydraulic conductivity.

The four different hydraulic conductivity methods were F-FHT, MI, L-FHT, and ST. The F-FHT head test took into account the entire VFBR, while the MI, L-FHT and ST were point measurements of the organic treatment media. The F-FHT measurements were considered to be the most comparable to the "true" hydraulic conductivity of the process unit, because it took into account every layer and the piping system of the cell. F-FHT hydraulic conductivity measurements ranged from $5.07x10^{-3}$ to $1.49x10^{-4}$ cm/s.

The MI was a new tool that was developed to measure the in situ hydraulic conductivity of the organic treatment media. No in situ direct measurements of the treatment media have been reported until this research. After field verifying the methodology, the MI method was able to produce repeatable results that were comparable to the F-FHT test and other methods. The measurements ranged from $9.96x10^{-4}$ to $1.04x10^{-4}$ cm/s.

The L-FHT tests were completed on the recovered cores from the MI tests. Since the L-FHT was testing the exact same material as the MI, it was expected that these two tests would yield similar results. The L-FHT measurements proved to be more variable than the other tests, which made the L-FHT measurements statistically comparable to the

MI measurements, but not as precise. The process of coring the substrate, and transporting of the cores from the field to the laboratory likely disturbed the hydraulic conductivity of the substrate. The L-FHT measurements ranged from $4.76x10^{-3}$ to $2.70x10^{-4}$ cm/s.

The ST tests were completed at the Red Oak and Mayer Ranch PTS, because piezometers and porewater samplers were installed during construction at these sites. The piezometer measurements at Red Oak PTS were considerably different from the other measurements in the cell. However, the porewater samplers were closer to the F-FHTs conducted at Mayer Ranch PTS. This is likely due to the construction method of the piezometers. The piezometers at the Red Oak PTS most likely were measuring the hydraulic conductivity of the sand pack rather than the treatment media. However, another explanation is that the different ST measure the hydraulic conductivity in different direction (i.e. vertical vs horizontal). The ST measurements ranged from $3.15x10^{-4}$ to $1.74x10^{-5}$ cm/s.

Each method examined proved useful, but each has limitations as well. The F-FHT is likely most comparable to the "true" value of the entire cell and is relatively easy to perform. Unfortunately, it takes a considerable amount of time to be able to repeat tests (i.e., more than a month) and does not identify the restricting layer. The MI is an accurate point measurement of the treatment media, however it takes a considerable amount of work to gather the measurement. L-FHT, are easy to perform, but are highly variable and may not be representative of in situ conditions. The ST, are easy to perform, however, depending on the construction, may not be representative of the treatment media. There is no method that will fit all sites, but depending on site variables, certain methods may be more accurate or viable than others.

Comparing the hydraulic conductivity to the treatment media characteristics determined only one reasonable trend, with a few other weak trends. As the particle density of the treatment media increased, the hydraulic conductivity decreased linearly. The porosity does show a trend with hydraulic conductivity, but the trend is not as strong as the particle density trend. When comparing the bulk density, moisture content, and loss on ignition to the hydraulic conductivity, weak trends were identified in these data.

Prior to this research, the only reported data that were available on the hydraulic conductivity of VFBRs in PTS were tracer studies completed on cells that were in operation for four years or less. These studies did not directly measure the hydraulic conductivity of the treatment media (Diaz-Goebes and Younger 2004; Wolkersdorfer et al. 2005; Watson et al. 2008) but rather estimated it based on other bulk hydraulic characteristics. This study provided hydraulic conductivity measurements of VFBRs that have been in operation for 8-15 years, using in situ measurements of the treatment media, and a comparison the hydraulic conductivity against a number of different treatment media characteristics.

Vertical flow bioreactors are important tools for the treatment AMD. However, the failure of these cells can happen long before the design life has been reached. The hydraulic conductivity of these systems can be used to identify the problems that lead to failure. The identification of the problem can lead to a better understanding of VFBR performance well as development of better design criteria to improve future systems.

5 References

Beard, D.C., and Weyl, P.K. (1973). Influence of texture on porosity and permeability of unconsolidated sand. *The American Association of Petroleum Geologists Bulletin, 57(2),* pp. 349-369.

Blake, G.R. and Hartge, K.H. (1986). Bulk density method. In *Methods of Soil Analysis. Part 1, Physical and Mineralogical Methods,* 2nd ed., Edited by A. Klute. pp. 363-375

Bouwer, H. and Rice, R. C. (1976). A slug test for determining hydraulic conductivity of unconfined aquifers with completely or partially penetrating wells. *Water Resources Research, 12*(3), pp. 423–428, Retrieved from http://doi.org/10.1029/WR012i003p00423

Bouwer, H. (1989). The Bouwer and Ride Slug Test – An Update. *Groundwater,* 27(3), pp. 298-411.

Damariscotta Inc. (2003). Operation and maintenance for passive treatment systems. Clarion, PA. pg. 32-38 Retrieved from http://www.amrclearinghouse.org/Sub/AMD treatment/OM%20Guidance%20Manual%20Damariscotta.pdf

Demchak, J., Morrow, T., & Skousen, J. (2001). Treatment of acid mine drainage by four vertical flow wetlands in Pennsylvania. *Geochemistry: Exploration, Environment, Analysis, 1*(1), pp. 71–80, Retrieved from http://doi.org/10.1144/geochem.1.1.71

Diaz-Goebes, M. and Younger, P. (2004) A simple analytical model for interpretation of tracer tests in two-domain subsurface flow systems. *Mine Water and the Environment. 23,* pp. *138-143.*

Dunn, M., Danehy, T., Neely, C., Mahony, R., Busler, S., and Denholm, C. (2014). Jennings passive treatment system rehabilitation. Abstract. Presented at the National Meeting of the American Society of Mining and Reclamation: *Exploring New Frontiers in Reclamation.* June 14-20 2014, Oklahoma City, OK.

Devlin, J. F., Schillig, P. C., Bowen, I., Critchley, C. E., Rudolph, D. L., Thomson, N. R., and Roberts, J. A. (2012). Applications and implications of direct groundwater velocity measurement at the centimeter scale. *Journal of Contaminant Hydrology*, *127*(1–4), pp. 3–14. Retrieved from http://doi.org/10.1016/j.jconhyd.2011.06.007

Doshi, S.M. (2006). Bioremediation of acid mine drainage using sulfate-reducing bacteria. National Network of Environmental Management, U.S. Environmental Protection Agency, Washington D.C. pp. 3-66

Denholm, C., Johnson, D., Taylor, W., Shearer, R., Danehy, T., Busler, S., and Dunn, M. (2010). Case study: "The Jennings System"- over a decade of successful passive treatment. Presented at the National Meeting of the American Society of Mining and

Reclamation: *Bridging Reclamation, Science and the Community.* June 5-11 2010, Pittsburgh, PA. pp. 154-169

Dvorak, D. H., Hedin, R. S., Edenborn, H. M., and McIntire, P. E. (1992). Treatment of metal-contaminated water using bacterial sulfate reduction: Results from pilot-scale reactors. *Biotechnology and Bioengineering*, *40*(5), pp. 609–616. Retrieved from http://doi.org/10.1002/bit.260400508

Fennessy, M. S., and Mitsch, W. J. (1989). Treating coal mine drainage with an artificial wetland. *Research Journal of the Water Pollution Control Federation*, *61*(11/12), 1691–1701. Retrieved from http://www.jstor.org/stable/41480392

Gazea, B., Adam, K., and Kontopoulos, A. (1996). A review of passive systems for the treatment of acid mine drainage. *Minerals Engineering*, *9*(1), pp. 23–42. Retrieved from http://doi.org/10.1016/0892-6875(95)00129-8

Gardner, W.H. (1986). Water Content Method. In *Methods of Soil Analysis. Part 1, Physical and Mineralogical Methods*, 2nd ed. Edited by A. Klute, pp. 493-544

Gee, G.W. and Bauder, J.W. (1986.) Particle-Size Analysis Method. In *Methods of Soil Analysis. Part 1, Physical and Mineralogical Methods*, 2nd ed. Edited by A. Klute, pp. 383-411

Google Earth A (2013) *Mayer Ranch PTS, 36°55'18.07" N, 94°52'19.74" W, elevation 792 ft* Viewed 20 October 2016. Retrieved from www.google.com/earth/index.html.

Google Earth B (2013) *Red Oak PTS, 34°56'01.30" N, 95°02'05.32" W, elevation 559 ft* Viewed 20 October 2016. Retrieved from www.google.com/earth/index.html.

Google Earth (2012) *Hartshorne PTS, 34°50'53.73" N, 95°30'06.41" W, elevation 687 ft* Viewed 20 October 2016. Retrieved from www.google.com/earth/index.html.

Gusek, J.J., Wildeman, T., Miller, A., Fricke, J. (1988). The challenges of designing, permitting and building a 1,200 gpm passive bioreactor for metal mine drainage Wet Fork Mine, Missouri. Paper presented at the National Meeting of the American Society of Mining and Reclamation: *Mining—Gateway to the Future!*. May 17-21, 1998 St. Louis Missouri. pp. 203-212

Gusek, J.J. (2002). Sulfate-reducing bioreactor design and operating issues: Is this the passive treatment technology for your mine drainage? Paper presented at the National Association of Abandoned Mine Land Programs. September 15-18, Park City Utah. pp. 533-547

Hedin, R. S., Watzlaf, G. R., and Nairn, R. W. (1994). Passive treatment of acid mine drainage with limestone. *Journal of Environment Quality*, *23*(6), pp. 1338-1345 Retrieved from http://doi.org/10.2134/jeq1994.00472425002300060030x

Hellier, W.W., and Hedin, R.S., (1992). The mechanism of iron removal from mine drainages by artificial wetlands at circumneutral pH. In: INTECOL IV International Wetlands Conference Abstracts, Columbus, OH, pp. 13

Hengen, T. J., Squillace, M. K., O'Sullivan, A. D., and Stone, J. J. (2014). Life cycle assessment analysis of active and passive acid mine drainage treatment technologies. *Resources, Conservation and Recycling*, *86*, 160–167 Retrieved from http://doi.org/10.1016/j.resconrec.2014.01.003

Jageman. T.C., Yokley, R.A., and Heunisch G.W. (1988). The use of pre-aeration to reduce the cost of neutralizing acid mine drainage. Paper presented at the National Meeting of the American Society of Mining and Reclamation: *Mine Drainage and Surface Mine Reclamation.* April 19-21, Pittsburgh, PA, pp. 131-135

Johnson, D. B., and Hallberg, K. B. (2005). Acid mine drainage remediation options: a review. *Science of the Total Environment*, *338*(1–2), 3–14 Retrieved from http://doi.org/10.1016/j.scitotenv.2004.09.002

Klute, A. and Dirksen, C. (1986). Hydraulic conductivity and diffusivity laboratory method. In *Methods of Soil Analysis. Part 1, Physical and Mineralogical Methods*, 2nd ed. Edited by A. Klute pp. 637-732

Letterman, R. D., and Mitsch, W. J. (1978). Impact of mine drainage on a mountain stream in Pennsylvania. *Environmental Pollution*, *17*(1), pp. 53–73 Retrieved from http://doi.org/10.1016/0013-9327(78)90055-1

Matthies, R., Aplin, A. C., and Jarvis, A. P. (2010). Performance of a passive treatment system for net-acidic coal mine drainage over five years of operation. *Science of the Total Environment*, *408*(20), pp. 4877–4885 Retrieved from http://doi.org/10.1016/j.scitotenv.2010.06.009

Nairn, R.W., LaBar, J.A., Strevett, K.A., Strosnider W.H., Morris, D., Garrido, A.E., Neely, C.A. and Kauk, K. (2010). Initial evaluation of a large multi-cell passive treatment system for net-alkaline ferruginous lean-zinc mine waters. Paper presented at the National Meeting of the American Society of Mining and Reclamation: *Bridging Reclamation, Science and the Community.* June 5-11 2010, Pittsburgh, PA, pp. 635-649

Neculita, C.-M., Zagury, G. J., and Bussière, B. (2007). Passive treatment of acid mine drainage in bioreactors using sulfate-reducing bacteria. *Journal of Environment Quality*, *36*(1), pp. 1-16, Retrieved from http://doi.org/10.2134/jeq2006.0066

Nelson, D.W., and Sommers, L.E. (1996). Loss-On-Ignition Method. In *Methods of Soil Analysis. Part 3, Chemical Methods*. Edited by D.L. Sparks pp. 1004-1005

Nordstrom, D. K., Alpers, C. N., Ptacek, C. J., and Blowes, D. W. (2000). Negative pH and extremely acidic mine waters from Iron Mountain, California. *Environmental Science and Technology*, *34*(2), pp. 254–258. Retrieved from http://doi.org/10.1021/es990646v

Nuttall, C. A., and Younger, P. L. (2000). Zinc removal from hard, circum-neutral mine waters using a novel closed-bed limestone reactor. *Water Research*, *34*(4), pp. 1262–1268. Retrieved from http://doi.org/10.1016/S0043-1354(99)00252-3

Sheoran, A. S., and Sheoran, V. (2006). Heavy metal removal mechanism of acid mine drainage in wetlands: A critical review. *Minerals Engineering*, *19*(2), pp. 105–116. Retrieved from http://doi.org/10.1016/j.mineng.2005.08.006

Stark, L.R. (1992). Assessing the longevity of a constructed wetland receiving coal mine drainage in eastern Ohio. INTECOL IV International Wetlands Conference Abstracts, Columbus, OH, pp. 13

Suneson, N. (2012). Arkoma Basin Petroleum – Past, Present, and Future. *The Journal of the Oklahoma City Geological Society 63(1).* pp. 38-70

Surridge, B., Baird, A., and Heathwatie, B. (2005) Evaluating the quality of hydraulic conductivity estimates from piezometer slug tests in peat. *Hydrological Processes 19(6).* pp. 1227-1244

U.S.D.A. Forest Service (1993). Acid mine drainage from mines on the national forests, a management challenge. Program Aid 1505, p.1-12

U.S. Environmental Protection Agency. (1996). Acid digestion of sediments, sludges, and soils, U.S. EPA SW-846, Office of Solid Waste, Washington, DC. Retrieved from http://www.epa.gov/osw/hazard/testmethods/sw846/pdfs/3050b.pdf

U.S. Environmental Protection Agency. (2006). Test methods for evaluating solid wastes, physical and chemical methods, U.S. EPA SW-846, Office of Solid Waste, Washington, DC. Retrieved from http://www.epa.gov/epaoswer/hazwaste/test/sw846.htm

Watson, I., Taylor, K., Sapsford, D., and Banks, D. (2008) Tracer testing to investigate hydraulic performance of a RAPS treating mine water in South Wales. Paper presentation at the International Conference on Acid Rock Drainage: *Securing the Future*. June 22-26, 2009 Skellefteå, Sweden. pp. 1-10

Watzlaf, G.R., Schroeder, K.T. and Kairies, C., (2000). Long-term performance of alkalinity producing passive systems for the treatment of mine drainage. In: W.L. Daniels and S.G. Richardson (Editors), Proceedings of the 17th Annual National Meeting of the American Society of Surface Mining and Reclamation, Tampa, Florida, pp. 262 - 274.

Weindorf, D.C. and Roger, W. (2003). Determining particle density in dairy manure compost. *Texas Journal of Agriculture and Natural Resources*, 16, pp. 60-63

Winfrey, B. K., Nairn, R. W., Tilley, D. R., and Strosnider, W. H. J. (2014). Emergy and carbon footprint analysis of the construction of passive and active treatment systems for net alkaline mine drainage. *Mine Water and the Environment*, pp. 1–11. Retrieved from http://doi.org/10.1007/s10230-014-0304-6

Wolkerdorder, C., Hasche, J., Gobël, P., and Younger, P. (2005) Tracer test in the Bowden Close Passive Treatment System (UK) – Preliminary Results. *Wissenschaftliche Mitteilungen, 28* pp. 87-92

Younger, P. L. (2000). Holistic remedial strategies for short- and long-term water pollution from abandoned mines. *Mining Technology*, *109*(3), pp. 210–218. Retrieved from http://doi.org/10.1179/mnt.2000.109.3.210

Younger, P. L., Wolkersdorfer, C., and ERMITE-Consortium. (2004). Mining impacts on the fresh water environment: Technical and managerial guidelines for catchment scale management. *Mine Water and the Environment*, *23*(1), pp. s2–s80. Retrieved from http://doi.org/10.1007/s10230-004-0028-0

Younger, P. L., Banwart, S. A., & Hedin, R. S. (2002). Active treatment of polluted mine waters. In *Mine Water* (pp. 271–309). Springer Netherlands. Retrieved from http://link.springer.com.ezproxy.lib.ou.edu/chapter/10.1007/978-94-010-0610-1_4

Ziemkiewicz, P. F., Skousen, J. G., Brant, D. L., Sterner, P. L., and Lovett, R. J. (1997). Acid mine drainage treatment with armored limestone in open limestone channels. *Journal of Environmental Quality*, *26*(4), pp. 1017. Retrieved from http://search.proquest.com/docview/197372946?accountid=12964

Ziemkiewicz, P. F., Skousen, J. G., and Simmons, J. (2003). Long-term performance of passive acid mine drainage treatment systems. *Mine Water and the Environment*, *22*(3), pp. 118–129. Retrieved from http://doi.org/10.1007/s10230-003-0012-0